



1 **Reduced growth with increased quotas of particulate organic and inorganic**  
2 **carbon in the coccolithophore *Emiliania huxleyi* under future ocean climate**  
3 **change conditions**

4

5

6 **Yong Zhang,<sup>1,4</sup> Sin éad Collins,<sup>2</sup> Kunshan Gao<sup>1,3,\*</sup>**

7

8

9 <sup>1</sup>State Key Laboratory of Marine Environmental Science and College of Ocean and  
10 Earth Sciences, Xiamen University, Xiamen, China

11 <sup>2</sup>Institute of Evolutionary Biology, School of Biological Sciences, University of  
12 Edinburgh, Edinburgh EH9 3FL, United Kingdom

13 <sup>3</sup>Co-Innovation Center of Jiangsu Marine Bio-industry Technology, Jiangsu Ocean  
14 University, Lianyungang, China

15 <sup>4</sup>College of Environmental Science and Engineering, and Fujian Key Laboratory of  
16 Pollution Control and Resource Recycling, Fujian Normal University, Fuzhou, China

17

18

19 Running head: Response of *E. huxleyi* to multiple drivers

20

21 \*Correspondence: Kunshan Gao (ksgao@xmu.edu.cn)

22

23 Keywords: CO<sub>2</sub>; coccolithophore; functional trait plasticity; light; multiple drivers;  
24 nutrients; ocean acidification; warming.

25



26 **Abstract**

27 Effects of ocean acidification and warming on marine primary producers can be  
28 modulated by other environmental factors, such as levels of nutrients and light. Here,  
29 we investigated the interactive effects of five oceanic environmental drivers ( $\text{CO}_2$ ,  
30 temperature, light, dissolved inorganic nitrogen and phosphate) on growth rate,  
31 particulate organic (POC) and inorganic (PIC) carbon quotas of the cosmopolitan  
32 coccolithophore *Emiliana huxleyi*. Population growth rate increased with increasing  
33 temperature (16 to 20 °C) and light intensities (60 to 240  $\mu\text{mol photons m}^{-2} \text{s}^{-1}$ ), but  
34 decreased with elevated  $p\text{CO}_2$  concentrations (370 to 960  $\mu\text{atm}$ ) and reduced  
35 availability of nitrate (24.3 to 7.8  $\mu\text{mol L}^{-1}$ ) and phosphate (1.5 to 0.5  $\mu\text{mol L}^{-1}$ ). POC  
36 quotas were predominantly enhanced by combined effects of increased  $p\text{CO}_2$  and  
37 decreased availability of phosphate. PIC quotas increased with decreased availability  
38 of nitrate and phosphate. Our results show that concurrent changes in nutrient  
39 concentrations and  $p\text{CO}_2$  levels predominantly affected growth, photosynthetic carbon  
40 fixation and calcification of *E. huxleyi*, and imply that plastic responses to progressive  
41 ocean acidification, warming and decreasing availability of nitrate and phosphate  
42 reduce population growth rate while increasing cellular quotas of particulate organic  
43 and inorganic carbon of *E. huxleyi*, ultimately affecting coccolithophore-related  
44 ecological and biogeochemical processes.

45

46

47

48

49

50



51 **1 Introduction**

52 Ocean acidification (OA), due to continuous oceanic absorption of anthropogenic CO<sub>2</sub>,  
53 is occurring alongside ocean warming. This in turn, leads to shoaling in the upper  
54 mixed layer (UML) and a consequent reduction in the upward transport of nutrients  
55 into the UML. These ocean changes expose phytoplankton cells within the UML to  
56 multiple simultaneous stressors or drivers, and organismal responses to these drivers  
57 can affect both trophic and biogeochemical roles of phytoplankton (see reviews by  
58 Boyd et al., 2015; Gao et al., 2019 and literatures therein). While most studies on the  
59 effects of ocean global climate changes on marine primary producers have focused on  
60 organismal responses to one, two or three environmental drivers, there is an  
61 increasing awareness of the need to measure the combined effects of multiple drivers  
62 (see reviews by Riebesell and Gattuso, 2015; Boyd et al., 2018; Gao et al., 2019;  
63 Kwiatkowski et al., 2019). For this purpose, several manipulative experimental  
64 approaches have been recommended (Boyd et al., 2018). One approach using many  
65 unique combinations of different numbers of drivers showed that both short and long-  
66 term growth responses were, on average, explained by the dominant single driver in a  
67 multi-driver environment, but this result relies on having many (>5) drivers with  
68 known or measured large-effect single drivers (Brennan and Collins, 2015; Brennan et  
69 al., 2017). For experiments with multiple drivers where interactions are likely to  
70 preclude making predictions from single drivers, where average responses are not the  
71 most informative ones, or where logistics preclude using a very large number of  
72 multi-driver environments, Boyd et al. (2010) suggested an ‘environmental cluster’  
73 method where key drivers (such as temperature, light intensity, nutrient concentration,  
74 CO<sub>2</sub> and Fe) are covaried within experiments, allowing the investigation of  
75 physiological responses of phytoplankton to concurrent changes of the clustered



76 drivers. This approach examines responses to projected overall environmental shifts  
77 rather than pulling apart the biological or statistical interactions between responses to  
78 individual drivers. To our knowledge, studies to date have employed such a driver  
79 clustering approach to investigate responses of diatoms *Fragilariopsis cylindrus*,  
80 *Thalassiosira pseudonana*, *Skeletonema costatum*, and the prymnesiophyte  
81 *Phaeocystis antarctica* to combinations of drivers projected for 2100 (Xu et al., 2014a;  
82 Xu et al., 2014b; Boyd et al., 2016).

83 An environmental cluster approach is especially useful when drivers are known to  
84 interact in terms of the organismal responses they elicit, as is the case for OA, light  
85 levels, and key nutrients acting on population growth rate and carbon fixation (Boyd  
86 et al., 2016). For example, in the cosmopolitan coccolithophore *Emiliana huxleyi*,  
87 interactive effects of OA and light showed that OA increased population growth rate  
88 and photosynthetic carbon fixation under low light, whereas it slightly lowered  
89 population growth rate and photosynthetic carbon fixation under high light  
90 (Zondervan et al., 2002; Kottmeier et al., 2016). In addition, photosynthetic carbon  
91 fixation was further enhanced by longer light exposure at high  $p\text{CO}_2$  levels  
92 (Zondervan et al., 2002). On the other hand, OA can exacerbate the negative impact  
93 of solar UV radiation on photosynthetic carbon fixation and calcification in *E. huxleyi*  
94 under nutrient-replete conditions (Gao et al., 2009), but can increase calcification  
95 (coccolith volume) and particulate organic carbon (POC) quota under phosphate-  
96 limited conditions (Leonardos and Geider, 2005; Müller et al., 2017), demonstrating  
97 that the effects of OA on calcification is likely nutrient-dependent. On the other hand,  
98 ocean warming, which occurs alongside OA, is known to increase coccolith length,  
99 POC, particulate organic nitrogen (PON) and inorganic carbon (PIC) production rates  
100 of several *E. huxleyi* strains (Rosas-Navarro et al., 2016; Feng et al., 2017). Warming



101 has also been shown to increase the optimal  $p\text{CO}_2$  levels for growth, POC and PIC  
102 production rates (Sett et al., 2014). In one case warming was found to compensate for  
103 the negative impact of OA on growth rate under low light intensity (Feng et al., 2008).  
104 Nevertheless, decreased photosynthetic carbon fixation and calcification at reduced  
105 carbonate saturation state (lowered  $\text{Ca}^{2+}$  concentrations) were exacerbated by  
106 warming treatment (Xu et al., 2011). Overall, there is strong evidence that  
107 understanding the plastic responses of this key calcifier to ocean changes requires  
108 investigating responses to the overall expected shift in the environment, in addition to  
109 the detailed studies to date on individual drivers, due to the sheer number of  
110 interactions between individual drivers on traits that affect the trophic and  
111 biogeochemical roles of *E.huxleyi*.

112 Despite known interactions among two- and three-way combinations of OA,  
113 temperature, light, phosphate levels and nitrogen levels, there have been few  
114 empirical studies investigating effects of the larger cluster projected for future surface  
115 ocean changes. The data to date show that interactions among drivers can affect both  
116 the direction and magnitude of trait changes in biogeochemically important taxa. In  
117 addition, based on single or two-driver studies, changes in temperature,  $p\text{CO}_2$ , light,  
118 dissolved inorganic nitrogen (DIN) and phosphate (DIP) in combination are predicted  
119 to affect primary productions (Barton et al., 2016; Monteiro et al., 2016; Boyd et al.,  
120 2018; Gao et al., 2019; Kwiatkowski et al., 2019). Understanding the trait-based  
121 responses of cocolithophores to future ocean changes is important for projections of  
122 changes in the biogeochemical roles of phytoplankton, such as biological carbon  
123 pump efficiency (Rost and Riebesell, 2004).

124 In order to understand the combined effects of  $p\text{CO}_2$ , temperature, light, dissolved  
125 inorganic nitrogen (DIN) and phosphate (DIP) on functional traits, we incubated



126 *Emiliana huxleyi* (Lohmann) under different combinations of environmental  
127 conditions that represented subsets of, and eventually the complete set of  
128 environments for, this environmental driver cluster. We recently examined the  
129 interactive effects of light intensity and CO<sub>2</sub> level on growth rate, POC and PIC  
130 quotas of *E. huxleyi* under nutrients replete, low DIN, or low DIP concentrations  
131 (Zhang et al., 2019). Light, CO<sub>2</sub>, DIN and DIP levels usually change simultaneously  
132 with temperature, and temperature modulated responses of *E. huxleyi* to other  
133 environmental drivers (Gafar and Schulz, 2018; Tong et al., 2019). In addition,  
134 warming or cooling can directly influence the activity of enzymes, thus directly  
135 modulating metabolic rates (Sett et al., 2014). Because of the overwhelming evidence  
136 that temperature can act as a general modulator of organismal responses, we use the  
137 present study to examine how the addition of temperature as a key driver in the  
138 environmental change cluster can modulate the combined effects of CO<sub>2</sub>, light and  
139 nutrients. We found that future ocean scenario treatments with OA, warming,  
140 increased light and reduced availability of nutrients led to lower growth rate and  
141 larger POC and PIC quotas of *E. huxleyi*.

142

## 143 **2 Materials and Methods**

### 144 **2.1 Experimental setup**

145 *Emiliana huxleyi* strain PML B92/11 was originally isolated from coastal waters off  
146 Bergen, Norway, and obtained from the Plymouth algal culture collection, UK. The  
147 average levels of *p*CO<sub>2</sub>, temperature, light, dissolved inorganic nitrate (DIN) and  
148 phosphate (DIP) were set up according to recorded data in Norwegian coastal waters  
149 during 2000 to 2007 and projected for 2100 in high-latitudes (Larsen et al., 2004;  
150 Locarnini et al., 2006; Omar et al., 2010; Boyd et al., 2015) (Table S1). *E. huxleyi* was



151 cultured with a 12 h/12 h light/dark cycle in thermo-controlled incubators in Aquil  
152 medium, which was prepared according to Sunda et al. (2005) with the addition of  
153 2200  $\mu\text{mol L}^{-1}$  bicarbonate to achieve the total alkalinity (TA) of 2200  $\mu\text{mol L}^{-1}$ . The  
154 experiment was conducted in five steps (Fig. 1). Considering ocean acidification and  
155 warming as the key drivers for ocean climate changes, we first established 4 “baseline”  
156 treatments where the  $p\text{CO}_2$  and temperature drivers were combined in a fully factorial  
157 way: low  $p\text{CO}_2$  + low temperature (LCLT), high  $p\text{CO}_2$  + low temperature (HCLT),  
158 low  $p\text{CO}_2$  + high temperature (LCHT), and high  $p\text{CO}_2$  + high temperature (HCHT).  
159 Since reduced availability of nutrients and increased light exposures are triggered by  
160 warming-enhanced stratification, we then added additional single or pairs of drivers to  
161 each of these “baseline” treatments (Fig. S1). In step 1, low light (LL) was added; in  
162 step 2, high light (HL) was added. HL was then maintained for the rest of the  
163 experiment. In step 3, low nitrogen was added and high phosphate levels were  
164 maintained (LNHP). In step 4, low phosphate was added and high nitrogen levels  
165 were restored (HNLP). In step 5, both nitrogen and phosphate were low (LNLP),  
166 respectively (Figs. 1 and S1). In all cases, the cells were acclimated to each unique  
167 stressor cluster for at least 14–16 generations before physiological and biochemical  
168 parameters were measured. Although this stepwise design introduces a historical  
169 effect, physiological traits are generally reported after 10 to 20 generations  
170 acclimation to OA treatment (Perrin et al., 2016; Tong et al., 2016; Li et al., 2017), so  
171 the historical effects here are similar to those that would be introduced with standard  
172 methods in other physiology studies (Tong et al., 2016; Zhang et al., 2019). Since  
173 individually reduced availability of nitrate or phosphate decreased growth, did not  
174 change POC quota, and enhanced PIC quota under optimal light intensity (HL in this  
175 study) in the same *E. huxleyi* strain (Zhang et al., 2019), we hypothesized that



176 combination of DIN and DIP limitation would result in similar trend under the  $p\text{CO}_2$   
177 and/or temperature combined treatments. Therefore, we added stepwise nitrate and/or  
178 phosphate drivers (Fig. 1).

179 For step 1,  $\text{NO}_3^-$  and  $\text{PO}_4^{3-}$  were modified to  $24 \mu\text{mol L}^{-1}$  and  $1.5 \mu\text{mol L}^{-1}$ ,  
180 respectively, which is the HNHP treatment in the synthetic seawater (Sunda et al.,  
181 2005) (Fig. S1). The seawater was dispensed into 4 glass bottles, and 2 bottles of  
182 seawater were placed at  $16^\circ\text{C}$  (LT) in an incubator (HP400G-XZ, Ruihua, Wuhan),  
183 and aerated for 24 h with filtered (PVDF  $0.22 \mu\text{m}$  pore size, Haining) air containing  
184  $400 \mu\text{atm}$  (LC) or  $1000 \mu\text{atm}$   $p\text{CO}_2$  (HC). Another 2 bottles of seawater were  
185 maintained at  $20^\circ\text{C}$  (HT) in the other chamber and also aerated with LC or HC air as  
186 described above. The dry air/ $\text{CO}_2$  mixture was humidified with deionized water prior  
187 to the aeration to minimize evaporation. The LCLT, HCLT, LCHT and HCHT  
188 seawaters (Figs. 1a and S1) were then filtered ( $0.22 \mu\text{m}$  pore size, Polycap 75 AS,  
189 Whatman) and carefully pumped into autoclaved 250 mL polycarbonate bottles  
190 (Nalgene, 4 replicate flasks for each of LCLT, HCLT, LCHT and HCHT, a total of 16  
191 flasks at the beginning of the experiment) with no headspace to minimize gas  
192 exchange. The flasks were inoculated at a cell density of about  $150 \text{ cells mL}^{-1}$ . The  
193 volume of the inoculum was calculated (see below) and the same volume of seawater  
194 was taken out from the bottles before inoculation. The samples were initially cultured  
195 at  $60 \mu\text{mol photons m}^{-2} \text{ s}^{-1}$  (LL) of photosynthetically active radiation (PAR)  
196 (measured using a PAR Detector, PMA 2132 from Solar Light Company) under  
197 LCLT, HCLT, LCHT and HCHT conditions for 8 generations (6 days) (d), and then  
198 the samples were diluted to their initial concentrations and grown for another 8  
199 generations (6 d) (Fig. 1a). Samples in culture bottles were mixed twice a day at 9:00  
200 a.m. and 5:00 p.m. At the end of the incubation, sub-samples were taken for



201 measurements of cell concentration, POC and TPC quotas, TA, pH and nutrient  
202 concentrations.

203 In step 2, samples grown under the previous conditions were transferred at the end  
204 of the cultures from 60 (LL) to 240  $\mu\text{mol photons m}^{-2} \text{s}^{-1}$  (HL) of PAR with initial  
205 cell concentrations of 150 cells  $\text{mL}^{-1}$ , and acclimated to the HL for 8 generations (5 d  
206 in 16 °C environment, 4 d in 20 °C environment) (Fig. 1b). The cultures were then  
207 diluted to achieve initial cell concentration and incubated at the HL for another 8  
208 generations (the fifth day in 16 °C environment and the fourth day in 20 °C  
209 environment) before sub-samples were taken for measurements.

210 In step 3, step 4 and step 5,  $\text{NO}_3^-$  and  $\text{PO}_4^{3-}$  concentrations were set to be 8  $\mu\text{mol L}^{-1}$   
211 and 1.5  $\mu\text{mol L}^{-1}$  for the LNHP treatment, and 24  $\mu\text{mol L}^{-1}$  and 0.5  $\mu\text{mol L}^{-1}$  for the  
212 HNLP treatment, and 8  $\mu\text{mol L}^{-1}$  and 0.5  $\mu\text{mol L}^{-1}$  for the LNLP treatment,  
213 respectively (Fig. 1c,d,e). The LCLT, HCLT, LCHT and HCHT were step 1  
214 conditions, now we are into step 3, 4 and 5. Under 240  $\mu\text{mol photons m}^{-2} \text{s}^{-1}$  (HL) of  
215 PAR, cell samples with an initial concentration of 150 cells  $\text{mL}^{-1}$  were transferred  
216 from HNHP condition (step 2) to LNHP conditions (step 3) and acclimated to LNHP  
217 conditions for 8 generations (5 d in 16 °C environment, 4 d in 20 °C environment)  
218 (Fig. 1c). The cultures were then diluted back to initial cell concentrations and  
219 incubated in the LNHP conditions (step 3) for a further 8 generations. On the last day  
220 of the incubation (the fifth day in 16 °C environment and the fourth day in 20 °C  
221 environment), sub-samples were taken for measurements of the parameters.

222 After that, cell samples were transferred stepwise from HNHP conditions (step 2,  
223 Fig. 1b) to HNLP conditions (step 4, Fig. 1d), then from HNLP conditions to LNLP  
224 conditions (step 5, Fig. 1e). Cell samples were acclimated for 8 generations at HNLP  
225 and LNLP conditions, respectively, and followed by another 8 generation incubations



226 for 4 d at HT and 5 d at LT. On the fourth day (for populations in high temperature  
227 environments) or the fifth day (for populations in low temperature environments),  
228 sub-samples were taken for measurements (Fig. 1d,e). At low nutrient concentrations,  
229 maximal cell concentrations were limited by nutrients (Rouco et al., 2013; Rokitta et  
230 al., 2016). To check whether cells sampled were in exponential growth at each  
231 nutrient level, we examined cell concentrations every day at LCHT, or LCLT and  
232 high light conditions (Fig. S2). We found that cell concentrations were in the  
233 exponential growth phase during the 1<sup>st</sup> and 5<sup>th</sup> days at HT, and during the 1<sup>st</sup> and 7<sup>th</sup>  
234 days at LT. In this study, we taken samples in the 4<sup>th</sup> day at HT and in the 5<sup>th</sup> day at  
235 LT, and thus cells sampled were in the exponential growth phase of *E. huxleyi*.

236 In the previous work (Zhang et al., 2019), we transferred *E. huxleyi* cells stepwise  
237 from 80  $\mu\text{mol photons m}^{-2} \text{s}^{-1}$  to 120  $\mu\text{mol photons m}^{-2} \text{s}^{-1}$ , then to 200  $\mu\text{mol photons}$   
238  $\text{m}^{-2} \text{s}^{-1}$ , to 320  $\mu\text{mol photons m}^{-2} \text{s}^{-1}$  and to 480  $\mu\text{mol photons m}^{-2} \text{s}^{-1}$  at both LC and  
239 HC levels under HNHP, LNHP or HNLP conditions, respectively. In this study, we  
240 transferred the same strain from LL to HL under HNHP condition, and then from  
241 HNHP to LNHP or HNLP, and from HNLP to LNLP under HL conditions under 4  
242 “baseline” CO<sub>2</sub> and temperature treatments, in an effort to elucidate interactive and  
243 combined effects of temperature, CO<sub>2</sub>, DIN and DIP (Table S2), in contrast the  
244 previous work carried out under constant temperature (Zhang et al., 2019).

245

## 246 **2.2 Nutrient concentrations and carbonate chemistry measurements**

247 In the first and last days of the incubations, 20 mL samples for determination of  
248 inorganic nitrogen and phosphate concentrations were taken at the same time using a  
249 filtered syringe (0.22  $\mu\text{m}$  pore size, Haining) and measured by using a scanning  
250 spectrophotometer (Du 800, Beckman Coulter) according to Hansen and Koroleff



251 (1999). The nitrate was reduced to nitrite by zinc cadmium reduction and then total  
252 nitrite concentration was measured. In parallel, 25 mL samples were taken for  
253 determination of total alkalinity (TA) after being filtered (0.22  $\mu\text{m}$  pore size, Syringe  
254 Filter) under moderate pressure using a pump (GM-0.5A, JINTENG) and stored in the  
255 dark at 4  $^{\circ}\text{C}$  for less than 7 d. TA was measured at 20  $^{\circ}\text{C}$  by potentiometric titration  
256 (AS-ALK1+, Apollo SciTech) according to Dickson et al. (2003). Samples for  $\text{pH}_T$   
257 (total scale) determinations were syringe-filtered (0.22  $\mu\text{m}$  pore size), and the bottles  
258 were filled from bottom to top with overflow and closed immediately without  
259 headspace. The  $\text{pH}_T$  was immediately measured at 20  $^{\circ}\text{C}$  by using a pH meter  
260 (Benchtop pH, Orion 8102BN) which was calibrated with buffers (Tris•HCl, Hanna)  
261 at pH 4.01, 7.00 and 10.00. Carbonate chemistry parameters were calculated from TA,  
262  $\text{pH}_T$ , phosphate (at 1.5  $\mu\text{mol L}^{-1}$  or 0.5  $\mu\text{mol L}^{-1}$ ), temperature (at 16  $^{\circ}\text{C}$  or 20  $^{\circ}\text{C}$ ), and  
263 salinity using the  $\text{CO}_2$  system calculation in MS Excel software (Pierrot et al., 2006).  
264  $K_1$  and  $K_2$ , the first and second carbonic acid constants, were taken from Roy et al.  
265 (1993).

266

### 267 **2.3 Cell concentration measurements**

268 In the last day of the incubation, ~25 mL samples (8 samples) were taken at the same  
269 time (about 1:00 p.m.). Cell concentration and cell diameter ( $D$ ) were measured using  
270 a Z2 Coulter Particle Count and Size Analyzer (Beckman Coulter). The diameter of  
271 detected particles was set to be 3 to 7  $\mu\text{m}$  in the instrument, which excludes detached  
272 coccoliths (Müller et al., 2012). Cell concentration was also measured by microscopy  
273 (ZEISS), and variation in measured cell concentration between two methods was  $\pm$   
274 7.9% (Zhang et al., 2019). Average growth rate ( $\mu$ ) was calculated for each replicate  
275 according to the equation:  $\mu = (\ln N_1 - \ln N_0) / d$ , where  $N_0$  was 150 cells  $\text{mL}^{-1}$  and  $N_1$



276 was the cell concentration in the last day of the incubation,  $d$  was the growth period in  
277 days. *E. huxleyi* cells were spherical and its cell volume with coccoliths was  
278 calculated according to the equation:  $V = 3.14 \times (4/3) \times (D/2)^3$ .

279

#### 280 **2.4 Total particulate (TPC) and particulate organic (POC) carbon measurements**

281 100 mL samples for determination of TPC and POC quotas were filtered onto GF/F  
282 filters (pre-combusted at 450 °C for 6 h) at the same time in each treatment. TPC and  
283 POC samples were stored in the dark at -20 °C. For POC measurements, samples  
284 were fumed with HCl for 12 h to remove inorganic carbon, and samples for TPC  
285 measurements were not treated with HCl. All samples were dried at 60 °C for 12 h,  
286 and analyzed using a Thermo Scientific FLASH 2000 CHNS/O elemental analyzer  
287 (Thermo Fisher, Waltham, MA). Particulate inorganic carbon (PIC) quota was  
288 calculated as the difference between TPC quota and POC quota. POC and PIC  
289 production rates were calculated by multiplying cellular contents with  $\mu$  ( $d^{-1}$ ),  
290 respectively. Variations in measured carbon content between the four replicates were  
291 calculated to be 1–24% in this study.

292

#### 293 **2.5 Data analysis**

294 Firstly, we examined the interactions of temperature,  $pCO_2$  and light under nutrient-  
295 replete (HNHP) conditions. Here, the effects of temperature,  $pCO_2$ , light intensity and  
296 their interaction on growth rate, POC and PIC quotas were tested using a three-way  
297 analysis of variance (ANOVA). Secondly, we examined the effects of nutrient  
298 limitation in the different  $pCO_2$  and temperature environments under the high light  
299 intensity (HL). Here, the effects of temperature,  $pCO_2$ , dissolved inorganic nitrogen  
300 (DIN), dissolved inorganic phosphate (DIP) and their interaction on growth rate, POC



301 and PIC quotas were tested using a four-way ANOVA. Finally, a one-way ANOVA  
302 was used to test the differences in growth rate, POC and PIC quotas between present  
303 (defined as low levels of  $p\text{CO}_2$ , temperature and light along with high levels of DIN  
304 and DIP (LC LT LL HN HP)) and future ocean (defined as higher levels of  $p\text{CO}_2$ ,  
305 temperature, and light along with low levels of DIN and DIP (HC HT HL LN LP))  
306 scenarios. A Tukey post hoc test was performed to identify the differences between  
307 two temperatures, two  $p\text{CO}_2$  levels, two DIN or two DIP treatments. Normality of  
308 residuals was conducted with a Shapiro-Wilk's test, and a Levene test was conducted  
309 graphically to test for homogeneity of variances. A generalized least squares (GLS)  
310 model was used to stabilize heterogeneity if variances were non-homogeneous. All  
311 statistical calculations were performed using *R* (R version 3.5.0).

312 In order to quantify the individual effect of nitrate concentration or phosphate  
313 concentration on the physiological and biochemical parameters, we calculated the  
314 change ratio ( $R$ ) of physiological rates according to the equation:  $R = |M_{\text{LNHP or HNLP}}$   
315  $- M_{\text{HNHP}}| / M_{\text{HNHP}}$ , where  $M_{\text{LNHP or HNLP or HNHP}}$  represents measured trait values in  
316 LNHP or HNLP or HNHP conditions, and the ' | ' denotes the absolute value  
317 (Schaum et al., 2013). We then calculated the expected growth rate, POC quota and  
318 PIC quota in LNLP conditions based on the measured trait values in HNHP  
319 conditions and the change ratios in LNHP and HNLP conditions according to a linear  
320 model:  $E_{\text{LNLP}} = (1 - R_{\text{LNHP}} - R_{\text{HNLP}}) \times M_{\text{HNHP}}$  for growth rate and POC quota;  $E_{\text{LNLP}} =$   
321  $(1 + R_{\text{LNHP}} + R_{\text{HNLP}}) \times M_{\text{HNHP}}$  for PIC quota (Brennan and Collins, 2015). We tested the  
322 significant differences between the expected trait values ( $E_{\text{LNLP}}$ ) and the measured  
323 trait values ( $M_{\text{LNLP}}$ ) in LNLP conditions by a one-way ANOVA (Fig. S3). We also  
324 calculated the extent of synergy between LNHP and HNLP on growth rate, POC



325 quota and PIC quota according to equation:  $S = |E_{LNLP} - M_{HNHP}| / M_{HNHP}$ . Please  
326 see the discussion section for more information.

327

### 328 **3 Results**

#### 329 **3.1 Carbonate chemistry parameters and nutrient concentrations**

330 During the incubations,  $pH_T$  values increased due to organismal activity by, on  
331 average,  $0.03 \pm 0.01$  in LCLT, by  $0.01 \pm 0.01$  in HCLT, by  $0.02 \pm 0.01$  in LCHT and  
332 by  $0.02 \pm 0.01$  in HCHT conditions (Fig. 1f–j; Table 1). Correspondingly, seawater  
333  $pCO_2$  concentrations decreased by  $8.8\% \pm 1.1\%$  in LCLT, by  $6.1\% \pm 4.4\%$  in HCLT,  
334 by  $6.6\% \pm 1.7\%$  in LCHT, and by  $5.4\% \pm 3.6\%$  in HCHT conditions, respectively  
335 (Fig. 1k–o; Table 1).

336 During the incubations, dissolved inorganic nitrogen (DIN) concentrations  
337 decreased by  $28.7\% \pm 6.7\%$  in HNHP and LL (Fig. 1p), by  $26.8\% \pm 5.9\%$  in HNHP  
338 and HL (Fig. 1q), by  $71.1\% \pm 3.3\%$  in LNHP (Fig. 1r), by  $32.9\% \pm 5.6\%$  in HNLP  
339 (Fig. 1s), and by  $69.8\% \pm 3.2\%$  in LNLP conditions (Fig. 1t; Table 2). Dissolved  
340 inorganic phosphate (DIP) concentrations decreased by  $62.2\% \pm 16.5\%$  in HNHP and  
341 LL (Fig. 1u), by  $71.3\% \pm 6.7\%$  in HNHP and HL (Fig. 1v), by  $61.0\% \pm 5.2\%$  in  
342 LNHP (Fig. 1w), by  $83.8\% \pm 5.4\%$  in HNLP (Fig. 1x), and by  $86.3\% \pm 1.4\%$  in LNLP  
343 conditions (Fig. 1y; Table 2).

344 Overall, while organismal activity affected nutrient levels during growth cycles as  
345 expected, the high and low nutrient treatments remained different at all times (Table  
346 2). Organismal activity had minimal effects on carbonate chemistry (see Fig. 1).

347

#### 348 **3.2 Population growth rate**



349 Growth rate was significantly lower under the future scenario (HCHT HL LNLP: high  
350 levels of  $p\text{CO}_2$ , temperature and light as well as low levels of nutrients) than under the  
351 present scenario (LCLT LL HNHP: low levels of  $p\text{CO}_2$ , temperature and light  
352 alongside high levels of nutrients) (one-way ANOVA,  $F = 52.6$ ,  $p < 0.01$ ) (Figs. 2a  
353 and 3a,d; Table 2). The effect of increasing  $p\text{CO}_2$  on growth rate is negative at low  
354 light or low nutrients levels, which can be seen by comparing population growth in all  
355 of the HC regimes with their paired LC regimes (Figs. 3a,b,e and S4). The extent of  
356 reduction in population growth rate depends on which other stressors are present.  
357 Compared to present atmospheric  $p\text{CO}_2$  levels (LC, Fig. 3a), growth rates under ocean  
358 acidification (HC, Fig. 3b) decreased by an average of  $17.4\% \pm 1.3\%$  in HNHP and  
359 LL, and by an average of  $4.4\% \pm 1.1\%$  in HNHP and HL conditions (three-way  
360 ANOVA, both  $p < 0.01$ ; Tukey post hoc test, both  $p < 0.01$ ) (Fig. 3e; Tables 2 and 3),  
361 by  $7.6\% \pm 2.6\%$  in LNHP, by  $21.4\% \pm 0.2\%$  in HNLP, and by  $32.1\% \pm 0.5\%$  in  
362 LNLP conditions under the HL, respectively (four-way ANOVA, all  $p < 0.01$ ; Tukey  
363 post hoc test, all  $p < 0.01$ ) (Fig. 3a,b,e; Tables 2 and 4).

364 Across all HT/LT (high/low temperature) regime pairs, population growth rate is  
365 faster in the HT regimes, indicating that increasing temperature from 16 to 20 °C  
366 increases population growth rate in *E. huxleyi* (Figs. 3a,c,f and S4). Compared to the  
367 low temperature (LT, Fig. 3a), growth rates at the high temperature (HT, Fig. 3c)  
368 increased by  $7.7\% \pm 0.7\%$  in HNHP and LL, and by  $34.0\% \pm 0.4\%$  in HNHP and HL  
369 conditions (three-way ANOVA, both  $p < 0.01$ ; Tukey post hoc test, both  $p < 0.01$ )  
370 (Fig. 3a,c,f; Tables 2 and 3), by  $42.4\% \pm 0.4\%$  in LNHP, by  $33.5\% \pm 0.5\%$  in HNLP,  
371 and by  $40.4\% \pm 3.1\%$  in LNLP conditions under HL (four-way ANOVA, all  $p < 0.01$ ;  
372 Tukey post hoc test, all  $p < 0.01$ ) (Fig. 3a,c,f; Tables 2 and 4). Compared to low  $p\text{CO}_2$   
373 and low temperature (LCLT, Fig. 3a), growth rates in high  $p\text{CO}_2$  and high



374 temperature environments (HCHT, Fig. 3d) increased by  $3.9\% \pm 0.9\%$  in HNHP and  
375 LL, and by  $31.1\% \pm 0.1\%$  in HNHP and HL conditions (three-way ANOVA, both  $p <$   
376  $0.01$ ; Tukey post hoc test, both  $p < 0.01$ ) (Fig. 3a,d,g; Tables 2 and 3), by  $38.6\% \pm 0.1\%$   
377 in LNHP and by  $17.1\% \pm 1.7\%$  in HNLP, whereas growth rate decreased by  $12.1\% \pm$   
378  $2.2\%$  in LNLP conditions under HL, respectively (four-way ANOVA, all  $p < 0.01$ ;  
379 Tukey post hoc test, all  $p < 0.01$ ) (Fig. 3a,d,g; Tables 2 and 4). These results show  
380 that high  $p\text{CO}_2$ , low nitrate and low phosphate concentrations collectively reduced the  
381 population growth rate in *E. huxleyi*, though elevated temperature could counteract  
382 this response.

383 The effects of reduced availability of nutrients on growth are nutrient-specific (Fig.  
384 3). Compared to HNHP and HL, growth rates in LNHP decreased by 3.0–12.1% (all  $p$   
385  $< 0.05$  at LCLT, HCLT, LCHT and HCHT conditions) (Fig. 3h; Tables 2 and 4). In  
386 contrast, HNLP did not significantly affect growth in LC conditions ( $p > 0.1$  in LCLT  
387 and LCHT conditions) (Fig. 3a,c,i), but did lower population growth rate by 11.3–  
388 19.2% in HC conditions (both  $p < 0.01$  at HCLT and HCHT conditions) (Fig. 3b,d,i).  
389 Unsurprisingly, when both nitrate and phosphate levels were reduced, growth rates  
390 always decreased by larger extent compared to environments where they were  
391 reduced individually (Fig. 3h,i,j). Compared to growth rates in HNHP and HL, growth  
392 rates in LNLP were 4.8–10.2% lower in LC environments, and 34.7–40.3% lower in  
393 HC environments (Tukey post hoc test, all  $p < 0.01$  at LCLT, HCLT, LCHT and  
394 HCHT conditions) (Fig. 3a–d,j; Tables 2 and 4). In summary, nitrate and phosphate  
395 limitation exacerbated the impacts of OA and warming on population growth rate.

396

### 397 **3.3 POC quota**



398 Cellular POC quotas were two-fold larger under the future scenario (HCHT HL LNLP)  
399 than under the current scenario (LCLT LL HNHP) (one-way ANOVA,  $F = 96.1$ ,  $p <$   
400  $0.01$ , Figs. 2b and 4a,d). The effect of increasing  $p\text{CO}_2$  on POC quota is positive,  
401 regardless of other drivers present, which can be seen by comparing POC quotas in all  
402 of the HC regimes with their paired LC regimes (Figs. 4a,b,e and S4), though the  
403 extent of increase in POC quota depends on which other stressors are present.  
404 Compared to current atmospheric  $p\text{CO}_2$  level (LC, Fig. 4a), POC quotas under ocean  
405 acidification (Fig. 4b) increased by  $40.3\% \pm 10.1\%$  in HNHP and LL (Tukey post hoc  
406 test,  $p < 0.01$ ), by  $13.8\% \pm 10.1\%$  in HNHP and HL ( $p = 0.47$ ), by  $33.2\% \pm 11.1\%$  at  
407 LNHP, by  $109.4\% \pm 14.0\%$  in HNLP and by  $87.3\% \pm 10.8\%$  in LNLP conditions  
408 under HL, respectively (four-way ANOVA, all  $p < 0.01$ ; Tukey post hoc test, all  $p <$   
409  $0.01$ ) (Fig. 4a,b,e; Tables 2 and 4).

410 The effect of elevated temperature on POC quota can be seen by comparing POC  
411 quota in all of the HT regimes with their paired LT regimes (Figs. 4a,c,f and S4).  
412 Across all HT/LT regime pairs, POC quotas did not show significant differences  
413 between the HT and LT regimes under HNHP and LL, HNHP and HL, LNHP, HNLP  
414 and LNLP conditions under HL, respectively (Tukey post hoc test, all  $p > 0.1$ ) (Fig.  
415 4a,c,f). This demonstrated that increasing temperature within the test range had no  
416 significant effect on POC quota. The combined effects of increasing  $p\text{CO}_2$  and  
417 temperature on POC quotas were nutrient dependent. Compared to low  $p\text{CO}_2$  and low  
418 temperature (LCLT, Fig. 4a), POC quotas at high  $p\text{CO}_2$  and high temperature (HCHT,  
419 Fig. 4d) did not show significant differences in HNHP and LL ( $p = 0.79$ ), in HNHP  
420 and HL ( $p = 0.99$ ), and in LNHP and HL ( $p = 0.99$ ), but increased by  $52.2\% \pm 20.6\%$   
421 in HNLP and by  $45.6\% \pm 14.8\%$  in LNLP conditions under HL (Tukey post hoc test,  
422 both  $p < 0.01$ ) (Fig. 4a,d,g; Tables 2 and 4). These data showed that high  $p\text{CO}_2$  and



423 low phosphate concentrations enhanced POC quotas of *E. huxleyi*, and that their  
424 combined effects were partly reduced by rising temperature.

425 The effects of nutrient reduction on POC quota are nutrient specific (Fig. 4).  
426 Compared to HNHP and HL, POC quotas in LNHP did not show a significant  
427 difference (all  $p > 0.1$  at LCLT, HCLT, LCHT and HCHT) (Fig. 4a–d,h; Tables 2 and  
428 4). At LC, POC quotas did not significantly differ between HNHP, HNLP and LNLP  
429 conditions (Tukey post hoc test, all  $p > 0.1$ ) (Fig. 4a,c,i,j). In contrast, in HC, they  
430 were 43.3–78.2% larger in HNLP or LNLP than in HNHP (all  $p < 0.01$ ) (Fig. 4b,d,i,j;  
431 Table 2).

432

### 433 3.4 PIC quota

434 Cellular PIC quotas were significantly larger in the future scenario with high levels of  
435  $p\text{CO}_2$ , temperature and light along with low nutrients concentrations, than PIC quotas  
436 in the present scenario with low levels of  $p\text{CO}_2$ , temperature and light along with  
437 relatively high nutrients concentrations (one-way ANOVA,  $F = 63.6$ ,  $p < 0.01$ ) (Figs.  
438 2c and 5a,d). The effect of increasing  $p\text{CO}_2$  on PIC quota is negative, regardless of  
439 presence of other drivers. By comparing PIC quota in all of the HC regimes with their  
440 paired LC regimes (Figs. 5a,b,e and S4), the effects of elevated  $p\text{CO}_2$  level are clear,  
441 though the extent of reduction in PIC quota depends on which other stressors are  
442 present. Compared to present atmospheric  $p\text{CO}_2$  levels (LC, Fig. 5a), PIC quotas  
443 under ocean acidification (Fig. 5b) are reduced by  $31.8\% \pm 17.1\%$  in HNHP and LL,  
444 by  $34.3\% \pm 10.0\%$  in HNHP and HL, by  $25.0\% \pm 3.8\%$  in LNHP, by  $22.8\% \pm 6.3\%$  in  
445 HNLP and by  $44.6\% \pm 0.9\%$  in LNLP conditions under HL, respectively (Tukey post  
446 hoc test, all  $p < 0.05$ ) (Fig. 5a,b,e; Tables 2–4). The extent of reduction in PIC quota  
447 is larger under LNLP conditions.



448 The effects of rising temperature on PIC quota were nutrient dependent, and can be  
449 seen by comparing PIC quotas in the HT regimes with those in their paired LT  
450 regimes (Figs. 5a,c,f and S4). Compared to low temperature (LT, Fig. 5a), PIC quotas  
451 at high temperature (HT, Fig. 5c) did not show significant differences in HNHP and  
452 LL, in HNHP and HL, in LNHP, and in HNLP conditions (Tukey post hoc test, all  $p >$   
453 0.05), whereas they decreased by  $27.9\% \pm 8.4\%$  in LNLP conditions under HL  
454 (Tukey post hoc test,  $p < 0.01$ ) (Fig. 5a,c,f; Tables 2–4). The combined effects of  
455 rising  $p\text{CO}_2$  and temperature on PIC quota are negative, regardless of which other  
456 drivers are present (Fig. 5a,d,g). Compared to low  $p\text{CO}_2$  and low temperature (LCLT,  
457 Fig. 5a), PIC quotas in high  $p\text{CO}_2$  and high temperature (HCHT, Fig. 5d) declined by  
458  $11.1\% \pm 10.9\%$  in HNHP and LL ( $p = 0.96$ ), by  $32.5\% \pm 2.4\%$  in HNHP and HL ( $p <$   
459  $0.01$ ), by  $42.2\% \pm 3.2\%$  in LNHP ( $p < 0.01$ ), by  $10.2\% \pm 7.7\%$  in HNLP ( $p = 0.92$ ),  
460 and by  $45.3\% \pm 5.9\%$  in LNLP conditions under HL, respectively ( $p < 0.01$ ) (Fig.  
461 5a,d,g; Table 2).

462 Effects of both nitrate and phosphate reduction on PIC quota are positive,  
463 regardless of levels of  $p\text{CO}_2$  and temperature for the range used here (Fig. 5h,i,j).  
464 Compared to HNHP and HL, PIC quotas were larger in LNHP (Tukey post hoc test,  $p$   
465  $< 0.01$  in LCLT, HCLT and LCHT conditions;  $p = 0.73$  at HCHT condition) (Fig. 5h),  
466 in HNLP, and in LNLP conditions, respectively (all  $p < 0.01$  at LCLT, HCLT, LCHT  
467 and HCHT conditions) (Fig. 5a–d,i,j; Table 2). In addition, PIC quotas were larger in  
468 LNLP than in HNLP conditions (Tukey post hoc test,  $p < 0.01$  in LCLT and HCLT  
469 conditions;  $p = 0.06$  in LCHT;  $p = 0.21$  in HCHT conditions) (Fig. 5a–d,i,j). These  
470 data showed that low nitrate and phosphate concentrations act synergistically to  
471 increase PIC quotas, which was moderated under the high  $p\text{CO}_2$ .

472



473 **3.5 PIC / POC value**

474 The ratio of PIC to POC (PIC/POC value) was not significantly different between the  
475 future scenario (HCHT HL LNLP) and the current scenario (LCLT LL HNHP) (one-  
476 way ANOVA,  $F = 0.3$ ,  $p = 0.60$ ) (Figs. 2d and 6a,d). The PIC / POC value followed  
477 the same trend as for PIC quotas described above. The effect of increasing  $p\text{CO}_2$  on  
478 PIC / POC value was negative, regardless of which other drivers were present (Figs.  
479 6a,b,e and S4), but the extent of reduction in PIC / POC value depended on presence  
480 of other drivers. Compared to current atmospheric  $p\text{CO}_2$  levels (LC, Fig. 6a), PIC /  
481 POC values under ocean acidification (HC, Fig. 6b) decreased by  $50.7\% \pm 18.2\%$  in  
482 HNHP and LL, by  $41.8\% \pm 15.4\%$  in HNHP and HL, by  $43.9\% \pm 5.8\%$  in LNHP, by  
483  $63.0\% \pm 4.2\%$  in HNLP, and by  $70.7\% \pm 2.0\%$  in LNLP conditions under HL,  
484 respectively (Tukey post hoc test, all  $p < 0.05$ ) (Fig. 6a,b; Table 2).

485 The effect of rising temperature on PIC / POC value was nutrient dependant (Figs.  
486 6a,c,f and S4). Compared to low temperature (LT, Fig. 6a), PIC / POC values at high  
487 temperature (HT, Fig. 6c) did not show significant differences in HNHP and LL, in  
488 HNHP and HL, in LNHP, and in LNLP conditions (Tukey post hoc test, all  $p > 0.1$ ),  
489 whereas they increased by  $39.0\% \pm 8.9\%$  in HNLP conditions (Tukey post hoc test,  $p$   
490  $= 0.006$ ) (Fig. 6a,c,f; Table 2). The combined effects of elevated  $p\text{CO}_2$  and  
491 temperature on PIC / POC values were negative (Fig. 6a,d,g). Relative to low  $p\text{CO}_2$   
492 and low temperature (LCLT, Fig. 6a), PIC / POC values at high  $p\text{CO}_2$  and high  
493 temperature (HCHT, Fig. 6d) did not show significant differences in HNHP and LL,  
494 and in HNHP and HL conditions (Tukey post hoc test, both  $p > 0.1$ ), but they  
495 decreased by  $39.9\% \pm 3.0\%$  in LNHP, by  $40.6\% \pm 5.8\%$  in HNLP, and by  $67.8\% \pm$   
496  $3.1\%$  in LNLP conditions under HL, respectively (Tukey post hoc test, all  $p < 0.01$ )  
497 (Fig. 6a,d,g; Table 2).



498 Across all LNHP/HNHP (low/high nitrate) regime pairs, PIC / POC values were  
499 higher in the LNHP regime (Fig. 6h), though the extent of increase in PIC / POC  
500 values depended on  $p\text{CO}_2$  or temperature levels. Compared to HNHP and HL, PIC /  
501 POC values in LNHP were about  $106.0\% \pm 13.0\%$  larger (Tukey post hoc test,  $p <$   
502  $0.05$  in LCLT and LCHT conditions;  $p > 0.05$  in HCLT and HCHT conditions) (Fig.  
503 6a–d, h; Table 2). The effect of phosphate on PIC / POC value also depended on  
504  $p\text{CO}_2$  levels (Fig. 6i). In LC, PIC / POC values were larger in HNLP than in HNHP ( $p$   
505  $= 0.22$  at LCLT;  $p < 0.05$  at LCHT conditions), and in LNLP than in LP ( $p < 0.01$  at  
506 LCLT;  $p = 0.09$  in LCHT conditions) (Fig. 6a,c). In HC conditions, PIC / POC values  
507 did not show significant differences among HNHP, HNLP and LNLP conditions  
508 (Tukey post hoc test, all  $p > 0.05$  in HCLT and HCHT conditions) (Fig. 6b,d; Table 2).

509

#### 510 **4 Discussion**

511 Understanding effects of multiple drivers is helpful for improving how  
512 coccolithophores are represented in models (Krumhardt et al., 2017). Responses of  
513 growth, POC and PIC quotas to ocean acidification have been shown to be modulated  
514 by temperature (Gafar and Schulz, 2018; Tong et al., 2019), light intensity or light  
515 period (light : dark cycle) (Jin et al., 2017; Bretherton et al., 2019), DIN or DIP  
516 concentrations (Müller et al., 2017), combinations of light intensity and nutrients  
517 availability (Zhang et al., 2019) (Table 5). Following up our previous study (Zhang et  
518 al., 2019), we added temperature as a key driver of 5 drivers (Table S2), and explored  
519 how temperature changes would modulate the combined effects of  $\text{CO}_2$ , light, DIN  
520 and DIP that we previously reported. Our data showed that a future ocean climate  
521 change cluster (increasing  $\text{CO}_2$ , temperature, and light levels along with decreasing  
522 DIN and DIP levels) can lower growth rate with increased POC and PIC quota per



523 cell (Fig. 2) as a result of plastic responses to the drivers. In contrast, observations of  
524 coccolithophore Chl *a* increased from 1990 to 2014 in the North Atlantic, and rising  
525 CO<sub>2</sub> and temperature has been associated with accelerated growth of  
526 coccolithophores since 1965 in the North Atlantic (Rivero-Calle et al., 2015;  
527 Krumhardt et al., 2016). Our results from laboratory experiments with multiple  
528 drivers experiment instead predicted a different trend with progressive ocean climate  
529 change, suggesting that some key elements of understanding phytoplankton responses  
530 to changing conditions that would enable researchers to connect laboratory studies  
531 and field observations are missing. It should also be noted that regional responses to  
532 ocean global changes could differ due to chemical and physical environmental  
533 differences and species and strain variability among different oceans or regions  
534 (Blanco-Ameijeiras et al., 2016; Gao et al., 2019), and that this could also explain  
535 discrepancies between experiments and observations.

536 The decreased availability of nitrate or phosphate individually reduced growth rate  
537 and increased PIC quota, respectively, in this experiment. Furthermore, under LNLP  
538 and high *p*CO<sub>2</sub> levels, measured growth rates were significantly lower than the  
539 expected values estimated on the basis of the values in LNHP and HNLP conditions  
540 (Fig. S3a). This indicates synergistic negative effects of LN and LP on growth rate, an  
541 evidence that colimitation of N and P is more severe than that by N or P alone. Here,  
542 the extent of synergy between LN and LP on growth rate was calculated to be  
543 8.6% ±2.8% at low temperature and to be 40.6% ±3.8% at high temperature (Fig. S3a),  
544 suggesting modulating effect of temperature on response of growth rate to nutrient  
545 limitations (Thomas et al., 2017). Similarly, at LNLP and low *p*CO<sub>2</sub> level, the  
546 measured PIC quota was significantly larger than the expected value (Fig. S3c),  
547 indicating synergistic positive effects of LN and LP on PIC quota, with the extent of



548 synergy being  $31.4\% \pm 3.9\%$  at low temperature. LN and LP did not synergistically act  
549 to reduce POC quota.

550 While there were always interactions among stressors, increased temperature itself  
551 sped up population growth to a relatively consistent value at high light, regardless of  
552 nutrient limitation, with statistically significant but small differences over the different  
553 nutrient regimes (Fig. 3f). Rising  $p\text{CO}_2$  level not only decreased the absolute values of  
554 growth rate, but also reduced the positive effect of high temperature on growth. In  
555 addition, elevated  $p\text{CO}_2$  also altered patterns of growth responses to changes in light  
556 and nutrient levels (Fig. 3e–g). Interestingly, low-pH inhibited growth to lesser extent  
557 under the high light than under low light (Fig. 3e; Table 2). One possible explanation  
558 for this could be that photosynthesis under the high light regime could generate more  
559 energy-conserving compounds, which results in faster  $p\text{CO}_2$  removal and counteracts  
560 the negative effects of low pH. This interaction between low pH and high light was  
561 also observed when *E. huxleyi* was grown under incident sunlight (Jin et al., 2017).

562 Increases in temperature reduced PIC quotas under some conditions (high light  
563 (HL), HL-LNHP and HL-LNLP) (Fig. 5f), suggesting that the ratio of N:P is  
564 important in modulating calcification under warming. One striking result is the  
565 consistent negative effect of high  $p\text{CO}_2$  on growth and PIC quota, regardless of other  
566 stressors. While  $p\text{CO}_2$  levels affected the absolute PIC values, the combination of  
567 high  $p\text{CO}_2$  and warming did not affect the responses to light and nutrients once the  
568 direct reduction in PIC quota due to increased  $p\text{CO}_2$  was taken into account (Fig. 5g).  
569 It has been documented that PIC quotas of *E. huxleyi* reduced at high  $p\text{CO}_2$  due to  
570 suppressed calcification (Riebesell and Tortell, 2011). This knowledge has been based  
571 on experiments under nutrient-replicate or constant conditions without consideration  
572 of multiple drivers. In this work, PIC quota of *E. huxleyi* under OA were raised with



573 increased light intensity and decreased availability of nutrients (Figs. 2 and 5). These  
574 results are consistent with other studies (Perrin et al., 2016; Jin et al., 2017), which  
575 reported that nutrient limitations enhanced calcification, and increased light levels can  
576 partially counteract the negative effects of OA on calcification. Our data also indicate  
577 that effects of ocean climate change on calcification of *E. huxleyi* are more complex  
578 than previously thought (Meyer and Riebesell, 2015). It is worth noting that the  
579 observed higher POC and PIC quotas under future ocean climate change scenario  
580 could be attributed to cell cycle arrest of a portion of the community (Vaulot et al.,  
581 1987). Decreased availabilities of nitrate and phosphate can extend the G1 phase  
582 where photosynthetic carbon fixation and calcification occurred, and lead to lower  
583 dark respiration which reduces carbon consumption (Vaulot et al., 1987; Müller et al.,  
584 2008; Gao et al., 2018).

585 Low phosphate concentrations can induce high affinity phosphate uptake in *E.*  
586 *huxleyi* (Riegman et al., 2000; Dyhrman and Palenik, 2003; McKew et al., 2015). This  
587 mechanism enables *E. huxleyi* to take up phosphate efficiently at low  $p\text{CO}_2$   
588 concentrations, so that no significant difference in growth rate was observed between  
589 HNLP and HNHP treatments (Fig. 3a,c). However, at high  $p\text{CO}_2$ , low phosphate  
590 concentration (HNLP) lowered growth of *E. huxleyi* relative to HNHP (Fig. 3a–d;  
591 Table 2). While the affinity of *E. huxleyi* for phosphate under different  $p\text{CO}_2$  levels  
592 has not been studied, the extra energetic cost of coping with stress from high  $p\text{CO}_2$   
593 could limit the energy available for the active uptake of phosphate. In addition, the  
594 activity of alkaline phosphatase, which might work to reuse released organic P,  
595 decreases at low pH (Rouco et al., 2013). Finally, the enlarged cell volume in HC and  
596 HNLP (or LNLP) conditions may further reduce nutrient uptake by cells due to  
597 reduced surface to volume ratios, and lower cell division rates (Fig. S5) (Finkel, 2001).



598 On the other hand, HNLP also affected expressions of genes related to nitrogen  
599 metabolism due to the tight stoichiometric coupling of nitrogen and phosphate  
600 metabolism (Rokitta et al., 2016). Decreased availability of nitrate further limited  
601 nitrogen metabolism of *E. huxleyi* (Rokitta et al., 2014), which lowered the overall  
602 biosynthetic activity and reduced cellular PON quotas (Fig. S10). These explain the  
603 synergistic inhibitions of low-pH, low-phosphate and low-nitrate on growth of *E.*  
604 *huxleyi* (Fig. 3).

605 POC quotas were larger at high  $p\text{CO}_2$  than at low  $p\text{CO}_2$  under all treatments (Fig. 4;  
606 Table 2), which could be a combined outcome of increased photosynthetic carbon  
607 fixation (Zondervan et al., 2002; Hoppe et al., 2011; Tong et al., 2019) and reduced  
608 cell division (present work), leading to pronounced increase of POC quotas in the  
609 cells grown under low phosphate (HNLP) and high  $p\text{CO}_2$  (Fig. 4). At HNLP and high  
610  $p\text{CO}_2$  levels, photosynthetic carbon fixation proceeds whereas cell division rate  
611 decreases (Figs. 3 and 4), so reallocation of newly produced particulate organic  
612 carbon (POC) could be slowed down (Vaulot et al., 1987). In this case, over-synthesis  
613 of cellular organic carbon might be released as dissolved organic carbon (DOC),  
614 which can coagulate to transparent exopolymer particles (TEP) and attach to cells  
615 (Biermann and Engel, 2010; Engel et al., 2015). When cells were filtered on GF/F  
616 filters, any TEP would not have been separated from the cells and would have  
617 contributed to the measured POC quota in this study. However, released organic  
618 compounds should be negligible, since they are usually photorespiration-dependent  
619 (Beardall, 1989; Obata et al., 2013).

620 Synthesis of RNA is large biochemical sinks for phosphate in *E. huxleyi* and other  
621 primary producers (Dyhrman, 2016). Compared to HNHP conditions, HNLP-grown  
622 cells had only 7.8% of total RNA (Fig. S11). This indicates that decreased availability



623 of phosphate strongly decreased RNA synthesis, which would consequently extend  
624 the interphase of the cell cycle where calcification occurs (Müller et al., 2008). This  
625 could explain why PIC quotas were enhanced by decreased phosphate availability  
626 (Fig. 5). Similarly, decreased availability of nitrate decreased protein (or PON)  
627 synthesis (Fig. S10), which can also block cells in the interphase of the cell cycle, and  
628 increase the time available for calcification in *E. huxleyi* (Vaulot et al., 1987).  
629 Consistently with this, lower rates of assimilation or organic matter production in *E.*  
630 *huxleyi* in LNHP than in HNHP treatments are consistent with more energy being  
631 reallocated to use for calcification (Nimer and Merrett, 1993; Xu and Gao, 2012).

632 Large PIC quotas of coccolithophores may facilitate accumulation of calcium  
633 carbonate in the deep ocean and increase the contribution of CaCO<sub>3</sub> produced by  
634 coccolithophores to calcareous ooze in the pelagic ocean (Hay, 2004). Due to CaCO<sub>3</sub>  
635 being more dense than organic carbon, larger PIC quotas may facilitate effective  
636 transport of POC to deep oceans, leading to vertical DIC or CO<sub>2</sub> gradients of seawater  
637 (Milliman, 1993; Ziveri et al., 2007). While the effects of global ocean climate  
638 changes on physiological processes of phytoplankton can be complex, our results  
639 promote our understanding on how a cosmopolitan coccolithophore responds to future  
640 ocean environmental changes through plastic trait change. While substantial  
641 evolutionary responses to multiple drivers may help further, our results imply that  
642 decreased phosphate availability along with progressive ocean acidification and  
643 warming in surface ocean may reduce the competitive capability of *E. huxleyi* in  
644 oligotrophic waters.

645

646

647



648 *Data availability.* The data are available upon request to the corresponding author

649 (Kunshan Gao).

650

651

652

653 *Author contributions.* YZ, KG designed the experiment. YZ performed this

654 experiment. All authors analysed the data, wrote and improved the manuscript.

655

656

657

658 *Competing interests.* The authors declare that they have no conflict of interest.

659

660

661

662 *Acknowledgements.* This study was supported by National Natural Science

663 Foundation of China (41720104005, 41806129, 41721005), and Joint Project of

664 National Natural Science Foundation of China and Shandong province (No.

665 U1606404).

666

667

668

669

670

671

672



673 **References**

- 674 Barton, A. D., Irwin, A. J., Finkel, Z. V., and Stock, C. A.: Anthropogenic climate  
675 change drives shift and shuffle in North Atlantic phytoplankton communities,  
676 Proc. Nat. Aca. Sci. USA, 113, 2964–2969, doi:10.1073/pnas.1519080113, 2016.
- 677 Beardall, J.: Photosynthesis and photorespiration in marine phytoplankton, Aquat.  
678 Bot., 34, 105–130, doi: 10.1016/0304-3770(89)90052-1, 1989.
- 679 Biermann, A., and Engel, A.: Effect of CO<sub>2</sub> on the properties and sinking velocity of  
680 aggregates of the coccolithophore *Emiliana huxleyi*, Biogeosciences, 7, 1017–  
681 1029, doi :10.5194/bg-7-1017-2010, 2010.
- 682 Blanco-Ameijeiras, S., Lebrato, M., Stoll, H. M., Iglesias-Rodriguez, D., Müller, M.  
683 N., Méndez-Vicente, A., and Oschlies, A.: Phenotypic variability in the  
684 coccolithophore *Emiliana huxleyi*, Plos ONE, 11, e0157697, doi:  
685 10.1371/journal.pone.0157697, 2016.
- 686 Borchard, C., Borges, A. V., Händel, N., and Engel, A.: Biogeochemical response of  
687 *Emiliana huxleyi* (PML B92/11) to elevated CO<sub>2</sub> and temperature under  
688 phosphorus limitation: A chemostat study, J. Exp. Mar. Biol. Ecol., 410, 61–71,  
689 doi: 10.1016/j.jembe.2011.10.004, 2011.
- 690 Boyd, P. W., Collins, S., Dupont, S., Fabricius, K., Gattuso, J. P., Havenhand, J.,  
691 Hutchins, D. A., Riebesell, U., Rintoul, M. S., Vichi, M., Biswas, H., Ciotti, A.,  
692 Gao, K., Gehlen, M., Hurd, C. L., Kurihara, H., McGraw, C. M., Navarro, J. M.,  
693 Nilsson, G. E., Passow, U., and Pörtner, H. O.: Experimental strategies to assess  
694 the biological ramifications of multiple drivers of global ocean change—A  
695 review, Global Change Biol., 24, 2239–2261, doi: 10.1111/gcb.14102, 2018.
- 696 Boyd, P. W., Dillingham, P. W., McGraw, C. M., Armstrong, E. A., Cornwall, C. E.,  
697 Feng, Y., Hurd, C. L., Gault-Ringold, M., Roleda, M. Y., Timmins-Schiffman,



- 698 E., and Nunn, B. L.: Physiological responses of a Southern Ocean diatom to  
699 complex future ocean conditions, *Nat. Clim. Change*, 6, 207–213, doi:  
700 10.1038/NCLIMATE2811, 2016.
- 701 Boyd, P. W., Lennartz, S. T., Glover, D. M., and Doney, S. C.: Biological  
702 ramifications of climate-change-mediated oceanic multi-stressors, *Nat. Clim.*  
703 *Change*, 5, 71–79, doi: 10.1038/nclimate2441, 2015.
- 704 Boyd, P. W., Strzepek, R., Fu, F., and Hutchins, D. A.: Environmental control of  
705 open-ocean phytoplankton groups: Now and in the future, *Limnol. Oceanogr.*, 55,  
706 1353–1376, doi: 10.4319/lo.2010.55.3.1353, 2010.
- 707 Brennan, G., and Collins, S.: Growth responses of a green alga to multiple  
708 environmental drivers, *Nat. Clim. Change*, 5, 892–897, doi:  
709 10.1038/nclimate2682, 2015.
- 710 Brennan, G., Colegrave, N., and Collins, S.: Evolutionary consequences of  
711 multidriver environmental change in an aquatic primary producer, *Proc. Nat. Aca.*  
712 *Sci. USA*, 114, 9930–9935, doi: 10.1073/pnas.1703375114, 2017.
- 713 Bretherton, L., Poulton, A. J., Lawson, T., Rukminasari, N., Balestreri, C., Schroeder,  
714 D., Mark Moore, C., and Suggett, D. J.: Day length as a key factor moderating  
715 the response of coccolithophore growth to elevated  $p\text{CO}_2$ , *Limnol. Oceanogr.*, 64,  
716 1284–1296, doi: 10.1002/lno.11115, 2019.
- 717 De Bodt, C., Van Oostende, N., Harlay, J., Sabbe, K., and Chou, L.: Individual and  
718 interacting effects of  $p\text{CO}_2$  and temperature on *Emiliana huxleyi* calcification:  
719 study of the calcite production, the coccolith morphology and the coccosphere  
720 size, *Biogeosciences*, 7, 1401–1412, doi: 10.5194/bg-7-1401-2010, 2010.



- 721 Dickson, A. G., Afghan, J. D., and Anderson, G. C.: Reference materials for oceanic  
722 CO<sub>2</sub> analysis: a method for the certification of total alkalinity, *Mar. Chem.*, 80,  
723 185–197, doi: 10.1016/S0304-4203(02)00133-0, 2003.
- 724 Dyrhman, S. T., and Palenik, B.: Characterization of ectoenzyme activity and  
725 phosphate-regulated proteins in the coccolithophorid *Emiliana huxleyi*, *J.*  
726 *Plankton Res.*, 25, 1215–1225, doi: 10.1093/plankt/fbg086, 2003.
- 727 Dyrhman, S. T.: Nutrients and their acquisition: phosphorus physiology in microalgae,  
728 in: *The physiology of microalgae*, edited by: Borowitzka, M. A., Beardall, J. and  
729 Raven, J. A., Springer, Heidelberg, 155–183, doi: 10.1007/978-3-319-24945-2,  
730 2016.
- 731 Engel, A., Borchard, C., Loginova, A. N., Meyer, J., Hauss, H., and Kiko, R.: Effects  
732 of varied nitrate and phosphate supply on polysaccharidic and proteinaceous gel  
733 particles production during tropical phytoplankton bloom experiments,  
734 *Biogeosciences*, 12, 5647–5665, doi: 10.5194/bg-12-5647-2015, 2015.
- 735 Feng, Y., Roleda, M. Y., Armstrong, E., Boyd, P. W., and Hurd, C. L.:  
736 Environmental controls on the growth, photosynthetic and calcification rates of a  
737 southern hemisphere strain of the coccolithophore *Emiliana huxleyi*, *Limnol.*  
738 *Oceanogr.*, 62, 519–540, doi: 10.1002/lno.10442, 2017.
- 739 Feng, Y., Warner, M. E., Zhang, Y., Sun, J., Fu, F., Rose, J. M., and Hutchins, D. A.:  
740 Interactive effects of increased pCO<sub>2</sub>, temperature and irradiance on the marine  
741 coccolithophore *Emiliana huxleyi* (Prymnesiophyceae), *Eur. J. Phycol.*, 43, 87–  
742 98, doi: 10.1080/09670260701664674, 2008.
- 743 Finkel, Z. V.: Light absorption and size scaling of light-limited metabolism in marine  
744 diatoms, *Limnol. Oceanogr.*, 46, 86–94, doi: 10.4319/lo.2001.46.1.0086, 2001.



- 745 Gafar, N. A., and Schulz, K. G.: A three-dimensional niche comparison of *Emiliana*  
746 *huxleyi* and *Gephyrocapsa oceanica*: reconciling observations with projections,  
747 *Biogeosciences*, 15, 3541–3560, doi: 10.5194/bg-15-3541-2018, 2018.
- 748 Gao, G., Xia, J., Yu, J., and Zeng, X.: Physiological response of a red tide alga  
749 (*Skeletonema costatum*) to nitrate enrichment, with special reference to inorganic  
750 carbon acquisition, *Mar. Environ. Res.*, 133, 15–23, doi:  
751 10.1016/j.marenvres.2017.11.003, 2018.
- 752 Gao, K., Beardall, J., Häder, D. P., Hall-Spencer, J. M., Gao, G., and Hutchins, D. A.:  
753 Effects of ocean acidification on marine photosynthetic organisms under the  
754 concurrent influences of warming, UV radiation, and deoxygenation, *Front. Mar.*  
755 *Sci.*, 6, 322, doi: 10.3389/fmars.2019.00322, 2019.
- 756 Gao, K., Ruan, Z., Villafañe, V. E., Gattuso, J., and Walter-Helbling, E.: Ocean  
757 acidification exacerbates the effect of UV radiation on the calcifying  
758 phytoplankton *Emiliana huxleyi*, *Limnol. Oceanogr.*, 54, 1855–1862, doi:  
759 10.4319/lo.2009.54.6.1855, 2009.
- 760 Hansen, H. P., and Koroleff, F.: Determination of nutrients, in: *Methods of seawater*  
761 *analysis*, edited by: Grasshoff, K., Kremling, K. and Ehrhardt, M., WILEY-VCH  
762 Publishers, ISBN: 3-527-29589-5, 1999.
- 763 Hay, W. W.: Carbonate fluxes and calcareous nannoplankton, in: *Coccolithophores:*  
764 *from molecular biology to global impact*, edited by: Thierstein, H. R. and Young,  
765 J. R., Springer, Berlin, 509–528, 2004.
- 766 Hoppe, C. J. M., Langer, G., and Rost, B.: *Emiliana huxleyi* shows identical  
767 responses to elevated pCO<sub>2</sub> in TA and DIC manipulations, *J. Exp. Mar. Biol.*  
768 *Ecol.*, 406, 54–62, doi: 10.1016/j.jembe.2011.06.008, 2011.



- 769 Jin, P., Ding, J. C., Xing, T., Riebesell, U., and Gao, K. S.: High levels of solar  
770 radiation offset impacts of ocean acidification on calcifying and non-calcifying  
771 strains of *Emiliana huxleyi*, Mar. Ecol. Prog. Ser., 568, 47–58, doi:  
772 10.3354/meps12042, 2017.
- 773 Kottmeier, D. M., Rokitta, S. D., and Rost, B.: Acidification, not carbonation, is the  
774 major regulator of carbon fluxes in the coccolithophore *Emiliana huxleyi*, New  
775 Phytol., 211, 126–137, doi: 10.1111/nph.13885, 2016.
- 776 Krumhardt, K. M., Lovenduski, N. S., Iglesias-Rodriguez, M. D., and Kleypas, J. A.:  
777 Coccolithophore growth and calcification in a changing ocean, Prog. Oceanogr.,  
778 171, 276–295, doi: 10.1016/j.pocean.2017.10.007, 2017.
- 779 Krumhardt, K. M., Lovenduski, N. S., Freeman, N. M., and Bates, N. R.: Apparent  
780 increase in coccolithophore abundance in the subtropical North Atlantic from  
781 1990 to 2014, Biogeosciences, 13, 1163–1177, doi: 10.5194/bg-13-1163-2016,  
782 2016.
- 783 Kwiatkowski, L., Aumont, O., and Bopp, L.: Consistent trophic amplification of  
784 marine biomass declines under climate change, Glob. Change Biol., 25, 218–229,  
785 doi: 10.1111/gcb.14468, 2019.
- 786 Larsen, A., Flaten, G. A. F., Sandaa, R., Castberg, T., Thyrrhaug, R., Erga, S. R.,  
787 Jacquet, S., and Bratbak, G.: Spring phytoplankton bloom dynamics in  
788 Norwegian coastal waters: Microbial community succession and diversity,  
789 Limnol. Oceanogr., 49, 180–190, doi: 10.4319/lo.2004.49.1.0180, 2004.
- 790 Leonardos, N., and Geider, R. J.: Elevated atmospheric carbon dioxide increases  
791 organic carbon fixation by *Emiliana huxleyi* (haptophyta), under nutrient-limited  
792 high-light conditions, J. Phycol., 41, 1196–1203, doi: 10.1111/j.1529-  
793 8817.2005.00152.x, 2005.



- 794 Li, W., Yang, Y., Li, Z., Xu, J., and Gao, K.: Effects of seawater acidification on the  
795 growth rates of the diatom *Thalassiosira (Conticribra) weissflogii* under  
796 different nutrient, light and UV radiation regimes, *J. Appl. Phycol.*, 29, 133–142,  
797 doi: 10.1007/s10811-016-0944-y, 2017.
- 798 Locarnini, R. A., Mishonov, A. V., Antonov, J. I., Boyer, T. P., and Garcia, H. E.:  
799 World ocean atlas 2005, V. 1: Temperature, edited by: Levitus, S., NOAA Atlas  
800 NESDIS 61. U. S. Government Printing Office, 123–134, 2006.
- 801 Matthiessen, B., Eggers, S. L., and Krug, S. A.: High nitrate to phosphorus regime  
802 attenuates negative effects of rising  $p\text{CO}_2$  on total population carbon  
803 accumulation, *Biogeosciences*, 9, 1195– 1203, doi: 10.5194/bg-9-1195-2012,  
804 2012.
- 805 McKew, B. A., Metodieva, G., Raines, C. A., Metodiev, M. V., and Geider, R. J.:  
806 Acclimation of *Emiliana huxleyi* (1516) to nutrient limitation involves precise  
807 modification of the proteome to scavenge alternative sources of N and P, *Environ.*  
808 *Microbiol.*, 17, 1–13, doi: 10.1111/1462-2920.12957, 2015.
- 809 Meyer, J., and Riebesell, U.: Reviews and syntheses: response of coccolithophores to  
810 ocean acidification: a meta-analysis, *Biogeosciences*, 12, 1671–1682, doi:  
811 10.5194/bg-12-1671-2015, 2015.
- 812 Milliman, J. D.: Production and accumulation of calcium carbonate in the ocean:  
813 budget of a nonsteady state, *Global Biogeochem. Cy.*, 7, 927–957, doi:  
814 10.1029/93GB02524, 1993.
- 815 Monteiro, F. M., Bach, L. T., Brownlee, C., Bown, P., Rickaby, R. E. M., Poulton, A.  
816 J., Tyrrell, T., Beaufort, L., Dutkiewicz, S., Gibbs, S., Gutowska, M. A., Lee, R.,  
817 Riebesell, U., Young, J., and Ridgwell, A.: Why marine phytoplankton calcify,  
818 *Sci. Adv.*, 2, 1–14, doi: 10.1126/sciadv.1501822, 2016.



- 819 Müller, M. N., Antia, A. N., and LaRoche, J.: Influence of cell cycle phase on  
820 calcification in the coccolithophore *Emiliana huxleyi*, *Limnol. Oceanogr.*, 53,  
821 506–512, doi: 10.4319/lo.2008.53.2.0506, 2008.
- 822 Müller, M. N., Beaufort, L., Bernard, O., Pedrotti, M. L., Talec, A., and Sciandra, A.:  
823 Influence of CO<sub>2</sub> and nitrogen limitation on the coccolith volume of *Emiliana*  
824 *huxleyi* (Haptophyta), *Biogeosciences*, 9, 4155–4167, doi: 10.5194/bg-9-4155-  
825 2012, 2012.
- 826 Müller, M. N., Trull, T. W., and Hallegraeff, G. M.: Independence of nutrient  
827 limitation and carbon dioxide impacts on the Southern Ocean coccolithophore  
828 *Emiliana huxleyi*, *The ISME J.*, 11, 1777–1787, doi: 10.1038/ismej.2017.53,  
829 2017.
- 830 Nimer, N. A., and Merrett, M. J.: Calcification rate in *Emiliana huxleyi* Lohmann in  
831 response to light, nitrate and availability of inorganic carbon, *New Phytol.*, 123,  
832 673–677, doi: 10.1111/j.1469-8137.1993.tb03776.x, 1993.
- 833 Obata, T., Schoenefeld, S., Krahnert, I., Bergmann, S., Scheffel, A., and Fernie, A. R.:  
834 Gas-chromatography mass-spectrometry (GC-MS) based metabolite profiling  
835 reveals mannitol as a major storage carbohydrate in the coccolithophorid alga  
836 *Emiliana huxleyi*, *Metabolites*, 3, 168–184, doi: 10.3390/metabo3010168, 2013.
- 837 Omar, A. M., Olsen, A., Johannessen, T., Hoppema, M., Thomas, H., and Borges, A.  
838 V.: Spatiotemporal variations of *f*CO<sub>2</sub> in the North Sea, *Ocean Sci.*, 6, 77–89, doi:  
839 10.5194/osd-6-1655-2009, 2010.
- 840 Perrin, L., Probert, I., Langer, G., and Aloisi, G.: Growth of the coccolithophore  
841 *Emiliana huxleyi* in light- and nutrient-limited batch reactors: relevance for the  
842 BIOSOPE deep ecological niche of coccolithophores, *Biogeosciences*, 13, 5983–  
843 6001, doi: 10.5194/bg-13-5983-2016, 2016.



- 844 Pierrot, D., Lewis, E., and Wallace, D. W. R.: MS Excel program developed for CO<sub>2</sub>  
845 system calculations, ORNL/CDIAC-105, Carbon Dioxide Information Analysis  
846 Centre, Oak Ridge National Laboratory, U.S., Department of Energy, doi:  
847 10.3334/CDIAC/otg.CO2SYS\_XLS\_CDIAC105a, 2006.
- 848 R version 3.5.0.: The R foundation for statistical computing platform: x86\_64-w64-  
849 mingw32/x64, 2018.
- 850 Riebesell, U., and Gattuso, J. P.: Lessons learned from ocean acidification research,  
851 Nat. Clim. Change, 5, 12–14, doi: 10.1038/nclimate2456, 2015.
- 852 Riebesell, U., and Tortell, P. D.: Effects of ocean acidification on pelagic organisms  
853 and ecosystems, in: Ocean acidification, edited by: Gattuso, J. P. and Hansson, L.,  
854 Oxford University Press, 99–121, 2011.
- 855 Riegman, R., Stolte, W., Noordeloos, A. A. M., and Slezak, D.: Nutrient uptake and  
856 alkaline phosphatase (EC 3:1:3:1) activity of *Emiliana huxleyi*  
857 (Prymnesiophyceae) during growth under N and P limitation in continuous  
858 cultures, J. Phycol., 36, 87–96, doi: 10.1046/j.1529-8817.2000.99023.x, 2000.
- 859 Rivero-Calle, S., Gnanadesikan, A., Del Castillo, C. E., Balch, W. M., and Guikema,  
860 S. D.: Multidecadal increase in North Atlantic coccolithophores and the potential  
861 role of rising CO<sub>2</sub>, Science, 350, 1533–1537, doi: 10.1126/science.aaa8026, 2015.
- 862 Rokitta, S. D., von Dassow, P., Rost, B., and John, U.: *Emiliana huxleyi* endures N-  
863 limitation with an efficient metabolic budgeting and effective ATP synthesis,  
864 BMC Genomics, 15, 1051–1064, doi: 10.1186/1471-2164-15-1051, 2014.
- 865 Rokitta, S. D., von Dassow, P., Rost, B., and John, U.: P- and N-depletion trigger  
866 similar cellular responses to promote senescence in eukaryotic phytoplankton,  
867 Front. Mar. Sci., 3, 109, doi: 10.3389/fmars.2016.00109, 2016.



- 868 Rosas-Navarro, A., Langer, G., and Ziveri, P.: Temperature affects the morphology  
869 and calcification of *Emiliana huxleyi* strains, *Biogeosciences*, 13, 2913–2926,  
870 doi: 10.5194/bg-13-2913-2016, 2016.
- 871 Rost, B., and Riebesell, U.: Coccolithophores and the biological pump: responses to  
872 environmental changes, in: *Coccolithophores : from molecular biology to global*  
873 *impact*, edited by: Thierstein, H. R. and Young, J. R., Springer, Berlin, 99–125,  
874 2004.
- 875 Rost, B., Zondervan, I., and Riebesell, U.: Light-dependent carbon isotope  
876 fractionation in the coccolithophorid *Emiliana huxleyi*, *Limnol. Oceanogr.*, 47,  
877 120–128, doi: 10.2307/3069125, 2002
- 878 Rouco, M., Branson, O., Lebrato, M., and Iglesias-Rodríguez, M.: The effect of  
879 nitrate and phosphate availability on *Emiliana huxleyi* (NZEH) physiology  
880 under different CO<sub>2</sub> scenarios, *Front. Microbiol.*, 4, 1–11, doi:  
881 10.3389/fmicb.2013.00155, 2013.
- 882 Roy, R. N., Roy, L. N., Vogel, K. M., Porter-Moore, C., Pearson, T., Good, C. E.,  
883 Millero, F. J., and Campbell, D. C.: Thermodynamics of the dissociation of boric  
884 acid in seawater at S 5 35 from 0 degrees C to 55 degrees C, *Mar. Chem.*, 44,  
885 243–248, doi: 10.1016/0304-4203(93)90206-4, 1993.
- 886 Schaum, E., Rost, B., Millar, A. J., and Collins, S.: Variation in plastic responses of a  
887 globally distributed picoplankton species to ocean acidification, *Nat. Clim.*  
888 *Change*, 3, 298–302, doi: 10.1038/NCLIMATE1774, 2013.
- 889 Sett, S., Bach, L. T., Schulz, K. S., Koch-Klavsen, S., Lebrato, M., and Riebesell, U.:  
890 Temperature modulates coccolithophorid sensitivity of growth, photosynthesis  
891 and calcification to increasing seawater pCO<sub>2</sub>, *PLoS One*, 9(2), e88308, doi:  
892 10.1371/journal.pone.0088308, 2014.



- 893 Sunda, W. G., Price, N. M., and Morel, F. M. M.: Trace metal ion buffers and their  
894 use in culture studies, in: Algal culturing techniques, edited by: Andersen, R. A.,  
895 Elsevier Academic Press, 53–59, 2005.
- 896 Thomas, M. K., Aranguren-Gassis, M., Kremer, C. T., Gould, M. R., Anderson, K.,  
897 Klausmeier, C. A., Litchman, E.: Temperature-nutrient interactions exacerbate  
898 sensitivity to warming in phytoplankton, *Global Change Biol.*, 23, 3269–3280,  
899 doi: 10.1111/gcb.13641, 2017.
- 900 Tong, S., Hutchins, D., and Gao, K.: Physiological and biochemical responses of  
901 *Emiliania huxleyi* to ocean acidification and warming are modulated by UV  
902 radiation, *Biogeosciences*, 16, 561–572, doi: 10.5194/bg-16-561-2019, 2019.
- 903 Tong, S., Hutchins, D., Fu, F., and Gao, K.: Effects of varying growth irradiance and  
904 nitrogen sources on calcification and physiological performance of the  
905 coccolithophore *Gephyrocapsa oceanica* grown under nitrogen limitation,  
906 *Limnol. Oceanogr.*, 61, 2234–2242, doi: 10.1002/lno.10371, 2016.
- 907 Vaultot, D., Olson, R. J., Merkel, S., and Chisholm, S. E.: Cell-cycle response to  
908 nutrient starvation in two phytoplankton species, *Thalassiosira weissflogii* and  
909 *Hymenomonas carterae*, *Mar. Biol.*, 95, 625–630, doi: 10.1007/BF00393106,  
910 1987.
- 911 Xu, J., Gao, K., Li, Y., and Hutchins, D. A.: Physiological and biochemical responses  
912 of diatoms to projected ocean changes, *Mar. Ecol. Prog. Ser.*, 515, 73–81, doi:  
913 10.3354/meps11026, 2014b.
- 914 Xu, K., Fu, F., and Hutchins, D. A.: Comparative responses of two dominant  
915 Antarctic phytoplankton taxa to interactions between ocean acidification,  
916 warming, irradiance, and iron availability, *Limnol. Oceanogr.*, 59, 1919–1931,  
917 doi: 10.4319/lo.2014.59.6.1919, 2014a.



- 918 Xu, K., and Gao, K.: Reduced calcification decreases photoprotective capability in the  
919 coccolithophorid *Emiliana huxleyi*, *Plant Cell Physiol.*, 53, 1267–1274, doi:  
920 10.1093/pcp/pcs066, 2012.
- 921 Xu, K., Gao, K., Villafañe, V. E., and Helbling, E. W.: Photosynthetic responses of  
922 *Emiliana huxleyi* to UV radiation and elevated temperature: roles of calcified  
923 coccoliths, *Biogeosciences*, 8, 1441–1452, doi: 10.5194/bg-8-1441-2011, 2011.
- 924 Zhang, Y., Fu, F., Hutchins, D. A., and Gao, K.: Combined effects of CO<sub>2</sub> level, light  
925 intensity and nutrient availability on the coccolithophore *Emiliana huxleyi*,  
926 *Hydrobiologia*, 842, 127–141, doi: 10.1007/s10750-019-04031-0, 2019.
- 927 Ziveri, P., deBernardi, B., Baumann, K., Stoll, H. M., and Mortyn, P. G.: Sinking of  
928 coccolith carbonate and potential contribution to organic carbon ballasting in the  
929 deep ocean, *Deep Sea Res.*, 54, 659–675, doi: 10.1016/j.dsr2.2007.01.006, 2007.
- 930 Zondervan, I., Rost, B., and Riebesell, U.: Effect of CO<sub>2</sub> concentration on the  
931 PIC/POC ratio in the coccolithophore *Emiliana huxleyi* grown under light-  
932 limiting conditions and different daylengths, *J. Exp. Mar. Biol. Ecol.*, 272, 55–70,  
933 doi: 10.1016/s0022-0981(02)00037-0, 2002.
- 934  
935  
936  
937  
938  
939  
940  
941  
942



943 **Figure Legends**

944 **Figure 1.** Four “baseline” environments were used where  $p\text{CO}_2$  and temperature  
945 (temp) were combined in all pairwise combinations: low  $p\text{CO}_2$  + low temp (LCLT,  
946  $\Delta$ ), high  $p\text{CO}_2$  + low temp (HCLT,  $*$ ), low  $p\text{CO}_2$  + high temp (LCHT,  $\square$ ) and high  
947  $p\text{CO}_2$  + high temp (HCHT,  $\circ$ ). Additional stressors were then added to each of the  
948 four “baseline” environments. In step 1, low light (LL) was added. In step 2, high  
949 light (HL) was added. HL was then maintained for the rest of the experiment. In step  
950 3, low nitrogen was added and high phosphate levels were restored (LNHP). In step 4,  
951 low phosphate was added and high nitrogen levels were restored (HNLP). In step 5,  
952 both nitrogen and phosphate were low (LNLP). At each step, we measured cell  
953 concentration (**a–e**), medium  $\text{pH}_T$  value (**f–j**), medium  $p\text{CO}_2$  level (**k–o**), dissolved  
954 inorganic nitrogen (DIN) (**p–t**) and phosphate (DIP) (**u–y**) concentrations in the media  
955 in the beginning and at the end of the incubations. Respectively, LC and HC represent  
956  $p\text{CO}_2$  levels of about 370 and 960  $\mu\text{atm}$ ; LT and HT 16 and 20  $^\circ\text{C}$ ; LL and HL 60 and  
957 240  $\mu\text{mol photons m}^{-2} \text{s}^{-1}$  of photosynthetically active radiation (PAR); HN and LN  
958 24.3 and 7.8  $\mu\text{mol L}^{-1} \text{NO}_3^-$  at the beginning of the incubation; HP and LP 1.5 and 0.5  
959  $\mu\text{mol L}^{-1} \text{PO}_4^{3-}$  at the beginning of the incubations. The samples were taken in the last  
960 day of the cultures in each treatment. The values were indicated as the means  $\pm$  sd of  
961 4 replicate populations for each treatment.

962

963 **Figure 2.** Growth rate (**a**), particulate organic (POC, **b**) and inorganic (PIC, **c**) carbon  
964 quotas, PIC / POC value (**d**) and cell volume (**e**) of *Emiliana huxleyi* grown under the  
965 present (defined as low levels of  $p\text{CO}_2$ , temperature and light along with high levels  
966 of nutrients) and the future (defined as higher levels of  $p\text{CO}_2$ , temperature, and light  
967 along with low levels of nutrients due to ocean acidification, warming and shoaling of



968 upper mixing layer) scenarios. Data were obtained after cells were acclimated to  
969 experimental conditions for 14–16 generations and means  $\pm$  sd of 4 replicate  
970 populations. Different letters (a, b) in each panel represent significant differences  
971 between future and present ocean conditions (Tukey Post hoc,  $p < 0.05$ ).

972

973 **Figure 3.** Growth rates of *E. huxleyi* grown in LCLT (a), HCLT (b), LCHT (c) and  
974 HCHT (d) conditions, and the ratio of growth rate at HC to LC (e), HT to LT (f),  
975 HCHT to LCLT (g), LNHP to HNHP (h), HNLP to HNHP (i) and LNLP to HNHP (j).  
976 Data were obtained after cells were acclimated to experimental conditions for 14–16  
977 generations and means  $\pm$  sd of 4 replicate populations. Horizontal lines in panels (e)–  
978 (j) showed the value of 1. Different letters (a, b, c, d) in panels (a)–(d) represent  
979 significant differences between different nutrient treatments (Tukey Post hoc,  $p <$   
980 0.05). Detailed experimental conditions were shown in Figure 1.

981

982 **Figure 4.** POC quota of *E. huxleyi* grown in LCLT (a), HCLT (b), LCHT (c) and  
983 HCHT (d) conditions, and the ratio of POC quota at HC to LC (e), HT to LT (f),  
984 HCHT to LCLT (g), LNHP to HNHP (h), HNLP to HNHP (i) and LNLP to HNHP (j).  
985 Data were obtained after cells were acclimated to experimental conditions for 14–16  
986 generations and means  $\pm$  sd of 4 replicate populations. Horizontal lines in panels (e)–  
987 (j) showed the value of 1. Different letters (a, b) in panels (a)–(d) represent significant  
988 differences between different nutrient treatments (Tukey Post hoc,  $p < 0.05$ ). Detailed  
989 experimental conditions were shown in Figure 1.

990

991 **Figure 5.** PIC quota of *E. huxleyi* grown in LCLT (a), HCLT (b), LCHT (c) and  
992 HCHT (d) conditions, and the ratio of PIC quota at HC to LC (e), HT to LT (f),



993 HCHT to LCLT (g), LNHP to HNHP (h), HNLP to HNHP (i) and LNLP to HNHP (j).  
994 Data were obtained after cells were acclimated to experimental conditions for 14–16  
995 generations and means  $\pm$  sd of 4 replicate populations. Horizontal lines in panels (e)–  
996 (j) showed the value of 1. Different letters (a, b, c) in panels (a)–(d) represent  
997 significant differences between different nutrient treatments (Tukey Post hoc,  $p <$   
998 0.05). Detailed experimental conditions were shown in Figure 1.

999

1000 **Figure 6.** PIC / POC value of *E. huxleyi* grown in LCLT (a), HCLT (b), LCHT (c)  
1001 and HCHT (d) conditions, and the ratio of (PIC / POC value) at HC to LC (e), HT to  
1002 LT (f), HCHT to LCLT (g), LNHP to HNHP (h), HNLP to HNHP (i) and LNLP to  
1003 HNHP (j). Data were obtained after cells were acclimated to experimental conditions  
1004 for 14–16 generations and means  $\pm$  sd of 4 replicate populations. Horizontal lines in  
1005 panels (e)–(j) showed the value of 1. Different letters (a, b, c) in panels (a)–(d)  
1006 represent significant differences between different nutrient treatments (Tukey Post  
1007 hoc,  $p <$  0.05). Detailed experimental conditions were shown in Figure 1.

1008

1009 **Figure S1.** Flow chart of the experimental processes. Detailed experimental  
1010 conditions were shown in Figure 1.

1011

1012 **Figure S2.** Representative curves for the time course for cell concentrations of *E.*  
1013 *huxleyi* under low  $p\text{CO}_2$  (LC), high (HT) or low (LT) temperatures, and high light  
1014 (HL) conditions with varying levels of nutrients: HNHP (a), LNHP (b), HNLP (c) and  
1015 LNLP (d), respectively. Arrow indicates the day when samples were taken in each  
1016 treatment. Data were means  $\pm$  sd of 4 replicate populations. Detailed experimental  
1017 conditions were shown in Figure 1.



1018

1019 **Figure S3.** Comparison of growth rate (a), POC quota (b) and PIC quota (c) between  
1020 the expected (calculated) values and the measured values under the LNLP treatments.  
1021 Different letters (a, b) in each “baseline” environment (LCLT, HCLT, LCHT or  
1022 HCHT) represent significant differences (Tukey Post hoc,  $p < 0.05$ ). Detailed  
1023 experimental conditions were shown in Figure 1.

1024

1025 **Figure S4.** Heatmap of the changes in growth rate, POC quota, PIC quota and  
1026 PIC:POC in each treatment. Values in the present scenario (LC LT LL HNHP) were  
1027 considered as the control. A minus sign indicates the reduction in these parameters.

1028

1029 **Figure S5.** Cell volume of *E. huxleyi* grown in LCLT (a), HCLT (b), LCHT (c) and  
1030 HCHT (d) conditions, and its correlation with POC quota (e) and PIC quota (f). Data  
1031 were obtained after cells were acclimated to experimental conditions for 14–16  
1032 generations and means  $\pm$  sd of 4 replicate populations in panels (a)–(d). Each point in  
1033 panels (e) and (f) indicates an individual replicate from all experiment. Different  
1034 letters (a, b, c) in panels (a)–(d) represent significant differences between different  
1035 nutrient treatments (Tukey Post hoc,  $p < 0.05$ ).

1036

1037 **Figure S6.** Normalized POC quota of *E. huxleyi* to cell volume in LCLT (a), HCLT  
1038 (b), LCHT (c) and HCHT (d) conditions. Data were obtained after cells were  
1039 acclimated to experimental conditions for 14–16 generations and means  $\pm$  sd of 4  
1040 replicate populations. Different letters (a, b) in each panel represent significant  
1041 differences between different nutrient treatments (Tukey Post hoc,  $p < 0.05$ ).

1042



1043 **Figure S7.** Normalized PIC quota of *E. huxleyi* to cell volume in LCLT (a), HCLT  
1044 (b), LCHT (c) and HCHT (d) conditions. Data were obtained after cells were  
1045 acclimated to experimental conditions for 14–16 generations and means  $\pm$  sd of 4  
1046 replicate populations. Different letters (a, b, c) in each panel represent significant  
1047 differences between different nutrient treatments (Tukey Post hoc,  $p < 0.05$ ).

1048

1049 **Figure S8.** POC production rate of *E. huxleyi* in LCLT (a), HCLT (b), LCHT (c) and  
1050 HCHT (d) conditions, and the ratio of POC production rate at HC to LC (e), HT to LT  
1051 (f), HCHT to LCLT (g), LNHP to HNHP (h), HNLP to HNHP (i) and LNLP to  
1052 HNHP (j). Data were obtained after cells were acclimated to experimental conditions  
1053 for 14–16 generations and means  $\pm$  sd of 4 replicate populations. Horizontal lines in  
1054 panels (e)–(j) showed the value of 1. Different letters (a, b, c) in panels (a)–(d)  
1055 represent significant differences between different nutrient treatments (Tukey Post  
1056 hoc,  $p < 0.05$ ).

1057

1058 **Figure S9.** PIC production rate of *E. huxleyi* in LCLT (a), HCLT (b), LCHT (c) and  
1059 HCHT (d) conditions, and the ratio of PIC production rate at HC to LC (e), HT to LT  
1060 (f), HCHT to LCLT (g), LNHP to HNHP (h), HNLP to HNHP (i) and LNLP to  
1061 HNHP (j). Data were obtained after cells were acclimated to experimental conditions  
1062 for 14–16 generations and means  $\pm$  sd of 4 replicate populations. Horizontal lines in  
1063 panels (e)–(j) showed the value of 1. Different letters (a, b, c) in panels (a)–(d)  
1064 represent significant differences between different nutrient treatments (Tukey Post  
1065 hoc,  $p < 0.05$ ).

1066



1067 **Figure S10.** PON quota of *E. huxleyi* in LCLT (a), HCLT (b), LCHT (c) and HCHT  
1068 (d) conditions, and the ratio of PON quota at HC to LC (e), HT to LT (f), HCHT to  
1069 LCLT (g), LNHP to HNHP (h), HNLP to HNHP (i) and LNLP to HNHP (j). Data  
1070 were obtained after cells were acclimated to experimental conditions for 14–16  
1071 generations and means  $\pm$  sd of 4 replicate populations. Horizontal lines in panels (e)–  
1072 (j) showed the value of 1. Different letters (a, b) in panels (a)–(d) represent significant  
1073 differences between different nutrient treatments (Tukey Post hoc,  $p < 0.05$ ).

1074

1075 **Figure S11.** Normalized RNA quota of *E. huxleyi* to POC quota in HNHP and HNLP  
1076 conditions. Data were obtained after cells were acclimated to experimental conditions  
1077 for 14–16 generations and means  $\pm$  sd of 4 replicate populations. Different letters (a, b)  
1078 represent significant differences between different nutrient treatments (Tukey Post  
1079 hoc,  $p < 0.05$ ).

1080

1081

1082

1083

1084

1085

1086

1087

1088

1089

1090

1091



1092 **Table 1.** Carbonate chemistry parameters at the end of the incubation. The values are  
 1093 means  $\pm$ sd of 4 replicate populations. LL and HL represent 60 and 240  $\mu\text{mol photons}$   
 1094  $\text{m}^{-2} \text{s}^{-1}$  of photosynthetically active radiation (PAR), respectively; HN and LN  
 1095 represent 24.3 and 7.8  $\mu\text{mol L}^{-1}$  DIN in the beginning of the incubation; HP and LP  
 1096 represent 1.5 and 0.5  $\mu\text{mol L}^{-1}$  DIP in the beginning of the incubation, respectively.

			$p\text{CO}_2$ ( $\mu\text{atm}$ )	pH (total scale)	TA ( $\mu\text{mol}$ $\text{L}^{-1}$ )	DIC ( $\mu\text{mol}$ $\text{L}^{-1}$ )	$\text{HCO}_3^-$ ( $\mu\text{mol}$ $\text{L}^{-1}$ )	$\text{CO}_3^{2-}$ ( $\mu\text{mol}$ $\text{L}^{-1}$ )	$\text{CO}_2$ ( $\mu\text{mol}$ $\text{L}^{-1}$ )
16	LL-	LC	371 $\pm$ 17	8.07 $\pm$ 0.02	2266 $\pm$ 19	2017 $\pm$ 9	1823 $\pm$ 6	180 $\pm$ 8	13.4 $\pm$ 0.6
	HNHP	HC	918 $\pm$ 21	7.73 $\pm$ 0.02	2248 $\pm$ 45	2149 $\pm$ 39	2027 $\pm$ 35	90 $\pm$ 5	33.3 $\pm$ 0.7
	HL-	LC	387 $\pm$ 22	8.06 $\pm$ 0.02	2297 $\pm$ 12	2050 $\pm$ 17	1857 $\pm$ 20	179 $\pm$ 6	14.0 $\pm$ 0.8
	HNHP	HC	972 $\pm$ 11	7.71 $\pm$ 0.01	2283 $\pm$ 34	2189 $\pm$ 31	2066 $\pm$ 29	88 $\pm$ 3	35.2 $\pm$ 0.4
	HL-	LC	393 $\pm$ 20	8.05 $\pm$ 0.02	2273 $\pm$ 9	2033 $\pm$ 3	1845 $\pm$ 9	174 $\pm$ 7	14.3 $\pm$ 0.7
	LNHP	HC	1012 $\pm$ 13	7.69 $\pm$ 0.01	2263 $\pm$ 28	2177 $\pm$ 25	2057 $\pm$ 24	84 $\pm$ 2	36.7 $\pm$ 0.5
	HL-	LC	395 $\pm$ 19	8.06 $\pm$ 0.02	2318 $\pm$ 5	2073 $\pm$ 12	1879 $\pm$ 16	179 $\pm$ 6	14.3 $\pm$ 0.7
	HNLP	HC	958 $\pm$ 63	7.70 $\pm$ 0.01	2205 $\pm$ 69	2117 $\pm$ 71	1999 $\pm$ 69	84 $\pm$ 1	34.7 $\pm$ 2.3
	HL-	LC	375 $\pm$ 24	8.06 $\pm$ 0.01	2181 $\pm$ 78	1947 $\pm$ 77	1767 $\pm$ 73	167 $\pm$ 3	13.6 $\pm$ 0.9
	LNLP	HC	1014 $\pm$ 46	7.68 $\pm$ 0.01	2198 $\pm$ 73	2118 $\pm$ 73	2002 $\pm$ 69	79 $\pm$ 2	36.7 $\pm$ 1.7
20	LL-	LC	349 $\pm$ 16	8.09 $\pm$ 0.02	2257 $\pm$ 14	1963 $\pm$ 4	1741 $\pm$ 6	210 $\pm$ 8	11.3 $\pm$ 0.5
	HNHP	HC	899 $\pm$ 40	7.74 $\pm$ 0.02	2257 $\pm$ 53	2130 $\pm$ 45	1994 $\pm$ 40	107 $\pm$ 7	29.0 $\pm$ 1.3
	HL-	LC	363 $\pm$ 11	8.08 $\pm$ 0.01	2281 $\pm$ 16	1990 $\pm$ 18	1770 $\pm$ 19	208 $\pm$ 2	11.7 $\pm$ 0.3
	HNHP	HC	947 $\pm$ 24	7.72 $\pm$ 0.01	2248 $\pm$ 21	2130 $\pm$ 19	1998 $\pm$ 18	102 $\pm$ 3	30.6 $\pm$ 0.8
	HL-	LC	362 $\pm$ 18	8.08 $\pm$ 0.02	2262 $\pm$ 12	1973 $\pm$ 13	1756 $\pm$ 16	206 $\pm$ 7	11.7 $\pm$ 0.6
	LNHP	HC	970 $\pm$ 10	7.71 $\pm$ 0.01	2271 $\pm$ 31	2155 $\pm$ 28	2021 $\pm$ 25	102 $\pm$ 3	31.4 $\pm$ 0.3
	HL-	LC	370 $\pm$ 14	8.08 $\pm$ 0.01	2314 $\pm$ 3	2023 $\pm$ 10	1800 $\pm$ 14	211 $\pm$ 4	12.0 $\pm$ 0.4
	HNLP	HC	946 $\pm$ 47	7.71 $\pm$ 0.01	2200 $\pm$ 72	2088 $\pm$ 72	1960 $\pm$ 68	98 $\pm$ 2	30.6 $\pm$ 1.5
	HL-	LC	350 $\pm$ 18	8.08 $\pm$ 0.01	2193 $\pm$ 71	1912 $\pm$ 68	1701 $\pm$ 63	200 $\pm$ 5	11.3 $\pm$ 0.6
	LNLP	HC	977 $\pm$ 59	7.70 $\pm$ 0.01	2192 $\pm$ 78	2086 $\pm$ 79	1959 $\pm$ 76	95 $\pm$ 2	31.6 $\pm$ 1.9

1097

1098

1099

1100

1101

1102

1103

1104

1105



1106 **Table 2.** Final nitrate and phosphate concentrations (N : P,  $\mu\text{mol L}^{-1}$ ), growth rate ( $\text{d}^{-1}$ )  
 1107  $^{-1}$ ), POC and PIC quotas ( $\text{pg C cell}^{-1}$ ), and PIC / POC value. Values in the brackets  
 1108 represent final DIN and DIP concentrations, and standard deviation of 4 replicate  
 1109 populations for growth rate, POC and PIC quotas, and PIC / POC value. Detailed  
 1110 information was shown in Table 1.

$p\text{CO}_2$	T	Light	Final N : P	Growth rate	POC quota	PIC quota	PIC/POC
LC	LT	LL	HNHP (17.1 : 0.7)	0.96 (0.012)	1.80 (0.14)	0.38 (0.09)	0.21 (0.07)
		HL	HNHP (17.3 : 0.5)	1.09 (0.006)	2.50 (0.28)	0.62 (0.05)	0.25 (0.05)
		HL	LNHP (2.5 : 0.6)	1.00 (0.013)	2.07 (0.25)	0.90 (0.02)	0.44 (0.05)
		HL	HNLP (15.4 : 0.1)	1.08 (0.006)	2.42 (0.08)	0.83 (0.04)	0.34 (0.01)
		HL	LNLP (2.4 : 0.1)	0.99 (0.003)	2.62 (0.25)	1.62 (0.14)	0.63 (0.11)
HC	LT	LL	HNHP (18.6 : 0.9)	0.79 (0.012)	2.52 (0.33)	0.26 (0.06)	0.10 (0.04)
		HL	HNHP (18.2 : 0.5)	1.04 (0.012)	2.85 (0.36)	0.41 (0.06)	0.15 (0.04)
		HL	LNHP (2.0 : 0.6)	0.92 (0.026)	2.75 (0.23)	0.68 (0.03)	0.25 (0.03)
		HL	HNLP (15.5 : 0.1)	0.85 (0.002)	5.06 (0.34)	0.64 (0.05)	0.13 (0.01)
		HL	LNLP (2.7 : 0.1)	0.67 (0.005)	4.91 (0.28)	0.90 (0.01)	0.18 (0.01)
LC	HT	LL	HNHP (16.6 : 0.3)	1.03 (0.006)	1.58 (0.11)	0.43 (0.02)	0.27 (0.01)
		HL	HNHP (17.3 : 0.3)	1.46 (0.004)	2.15 (0.28)	0.52 (0.07)	0.25 (0.06)
		HL	LNHP (2.1 : 0.5)	1.42 (0.004)	1.68 (0.05)	0.79 (0.04)	0.47 (0.03)
		HL	HNLP (17.0 : 0.1)	1.44 (0.004)	2.09 (0.03)	1.00 (0.05)	0.48 (0.03)
		HL	LNLP (2.1 : 0.1)	1.39 (0.038)	2.02 (0.05)	1.17 (0.13)	0.58 (0.07)
HC	HT	LL	HNHP (16.7 : 0.4)	0.99 (0.008)	1.54 (0.12)	0.34 (0.05)	0.22 (0.04)
		HL	HNHP (17.9 : 0.5)	1.43 (0.001)	2.57 (0.06)	0.42 (0.02)	0.16 (0.01)
		HL	LNHP (2.4 : 0.6)	1.38 (0.009)	1.97 (0.03)	0.52 (0.03)	0.27 (0.01)
		HL	HNLP (17.1 : 0.1)	1.27 (0.018)	3.68 (0.50)	0.74 (0.06)	0.20 (0.02)
		HL	LNLP (2.2 : 0.1)	0.87 (0.022)	3.81 (0.39)	0.89 (0.10)	0.20 (0.04)

1111

1112

1113

1114

1115

1116

1117

1118



1119 **Table 3.** Results of three-way ANOVAs of the effects of temperature (T),  $p\text{CO}_2$  (C)  
 1120 and light intensity (L) and their interaction on growth rate, POC and PIC quotas, and  
 1121 PIC / POC value. Significant values were marked in bold.

		T	C	L	T×C	T×L	C×L	T×C×L
Growth rate	F	20037.5	477.4	23625.8	120.0	1550.9	34.0	86.4
	<i>p</i>	<b>&lt;0.01</b>						
POC quota	F	27.1	54.4	62.0	7.4	1.9	< 0.1	6.1
	<i>p</i>	<b>&lt;0.01</b>	<b>&lt;0.01</b>	<b>&lt;0.01</b>	<b>0.01</b>	0.18	0.83	<b>0.02</b>
PIC quota	F	0.4	38.6	47.6	2.3	6.6	1.6	1.1
	<i>p</i>	0.56	<b>&lt;0.01</b>	<b>&lt;0.01</b>	0.14	<b>0.02</b>	0.22	0.31
PIC / POC value	F	9.9	443.6	2.0	0.8	10.0	0.6	0.3
	<i>p</i>	<b>&lt;0.01</b>	<b>&lt;0.01</b>	0.17	0.38	<b>&lt;0.01</b>	0.46	0.60

1122

1123

1124

1125

1126

1127

1128

1129

1130

1131

1132

1133

1134

1135

1136

1137

1138

1139



1140 **Table 4.** Results of four-way ANOVAs of the effects of temperature (T),  $p\text{CO}_2$  (C),  
 1141 dissolved inorganic nitrate (N) and phosphate (P) concentrations and their interaction  
 1142 on growth rate, POC and PIC quotas, and PIC / POC value. Significant values were  
 1143 marked in bold.

	Growth rate		POC quota		PIC quota		PIC / POC value	
	F	<i>p</i>	F	<i>p</i>	F	<i>p</i>	F	<i>p</i>
T	500026.0	< <b>0.01</b>	297.4	< <b>0.01</b>	30.2	< <b>0.01</b>	82.8	< <b>0.01</b>
C	5798.0	< <b>0.01</b>	162.8	< <b>0.01</b>	376.2	< <b>0.01</b>	787.3	< <b>0.01</b>
N	4542.0	< <b>0.01</b>	157.0	< <b>0.01</b>	84.4	< <b>0.01</b>	127.6	< <b>0.01</b>
P	5347.0	< <b>0.01</b>	206.5	< <b>0.01</b>	474.6	< <b>0.01</b>	0.1	0.74
T×C	6899.0	< <b>0.01</b>	52.2	< <b>0.01</b>	0.2	0.68	7.2	< <b>0.01</b>
T×N	510.0	< <b>0.01</b>	5.6	<b>0.02</b>	60.0	< <b>0.01</b>	7.9	< <b>0.01</b>
T×P	39.0	< <b>0.01</b>	5.2	<b>0.03</b>	9.4	< <b>0.01</b>	16.2	< <b>0.01</b>
C×N	1265.0	< <b>0.01</b>	107.2	< <b>0.01</b>	9.5	< <b>0.01</b>	3.1	0.09
C×P	1718.0	< <b>0.01</b>	174.1	< <b>0.01</b>	14.7	< <b>0.01</b>	88.0	< <b>0.01</b>
N×P	179.0	< <b>0.01</b>	19.7	< <b>0.01</b>	10.7	< <b>0.01</b>	14.3	< <b>0.01</b>
T×C×N	35.0	< <b>0.01</b>	<0.1	0.81	0.2	0.67	1.9	0.17
T×C×P	27.0	< <b>0.01</b>	5.5	<b>0.02</b>	0.1	0.71	1.0	0.31
T×N×P	96.0	< <b>0.01</b>	<0.1	0.80	15.7	< <b>0.01</b>	3.3	0.08
C×N×P	241.0	< <b>0.01</b>	0.4	0.56	8.2	< <b>0.01</b>	1.2	0.28
T×C×N×P	105.0	< <b>0.01</b>	3.9	0.05	22.4	< <b>0.01</b>	4.5	<b>0.04</b>

1144  
 1145  
 1146  
 1147  
 1148  
 1149  
 1150  
 1151  
 1152  
 1153  
 1154  
 1155  
 1156  
 1157



1158 **Table 5.** List of the physiological responses of *E. huxleyi* to the concurrent changes in  
 1159 multiple drivers investigated by the laboratory incubations in the published studies. ‘↑’  
 1160 represents increase, ‘↓’ represents decrease, and ‘n’ represents no significant change  
 1161 to simultaneous changes in multiple drivers. C, T, L, N, P and  $\mu$  represent CO<sub>2</sub> ( $\mu$ atm),  
 1162 temperature (°C), light intensity ( $\mu$ mol photons m<sup>-2</sup> s<sup>-1</sup>), dissolved inorganic nitrogen  
 1163 and phosphate ( $\mu$ mol L<sup>-1</sup>), and growth rate, respectively. Simultaneous changes in  
 1164 multiple drivers were marked in bold. [1] represents De Bodt et al., (2010), [2]  
 1165 Borchard et al., (2011), [3] Sett et al., (2014), [4] Gafar and Schulz, (2018), [5] Tong  
 1166 et al., (2019), [6] Jin et al., (2017), [7] Bretherton et al., (2019), [8] Rost et al., (2002),  
 1167 [9] Feng et al., (2008), [10] Müller et al. (2012), [11] Perrin et al., (2016), [12]  
 1168 Leonardos and Geider, (2005), [13] Matthiessen et al., (2012), [14] Zhang et al.,  
 1169 (2019), [15] this study.

Strain	C	T	L	N	P	$\mu$	POC	PIC	PIC: POC	Cite
AC481	<b>380 to 750</b>	<b>13 to 18</b>	150	32	1	n	↑	↓	↓	[1]
PML B92/11	<b>300 to 900</b>	<b>14 to 18</b>	300	29	1	↑	n	↓	↓	[2]
PML B92/11	<b>400 to 1000</b>	<b>10 to 20</b>	150	64	4	↑	↑	↓	↓	[3]
PML B92/11	<b>400 to 1000</b>	<b>10 to 20</b>	150	64	4	↑	↓	↓		[4]
PML B92/11	<b>400 to 1000</b>	<b>15 to 24</b>	190	100	10	↑	↑	↓	↓	[5]
CCMP2090	<b>395 to 1000</b>	20	<b>57 to 567</b>	110	10	↑	↑			[6]
NZEH	<b>390 to 1000</b>	20	<b>175 to 300</b>	100	10	↓	↑	↑	↑	[7]
PCC124-3	<b>390 to 1000</b>	20	<b>175 to 300</b>	100	10	↑	n	↑	↑	[7]
PCC70-3	<b>390 to 1000</b>	20	<b>175 to 300</b>	100	10	↑	n	↑	↑	[7]
PML B92/11	<b>140 to 880</b>	15	<b>80 to 150</b>	100	6	↑	↑	↓	↓	[8]
PML B92/11	<b>395 to 1000</b>	20	<b>54 to 457</b>	110	10	↑	↑	↓	↓	[6]
PML B92/11	<b>400 to 1000</b>	20	<b>50 to 1200</b>	64	4	↑	↑	↑		[4]
RCC962	<b>390 to 1000</b>	20	<b>175 to 300</b>	100	10	↓	↑	n	↓	[7]
CCMP371	<b>375 to 750</b>	<b>20 to 24</b>	<b>50 to 400</b>	100	10	↑	n	↓	↓	[9]
B62	<b>280 to 1000</b>	20	300	<b>88 to 9</b>	4		↑	↓	↓	[10]
RCC911	400	20	<b>30 to 140</b>	<b>100 to 5</b>	6	↑	↑	↑	↑	[11]
RCC911	400	20	<b>30 to 140</b>	100	<b>6 to 0.6</b>	↑	↑	↑	↑	[11]



PML92A	<b>360 to 2000</b>	18	<b>80 to 500</b>	200	<b>6.7 to 40</b>	n	↑			[12]	
A	<b>460 to 1280</b>	16	130	<b>17 to 9</b>	<b>0.2 to 0.5</b>		↓	↓		[13]	
PML B92/11	<b>410 to 920</b>	20	<b>80 to 480</b>	<b>100 to 8</b>	10		↓	↓	↑	↑	[14]
PML B92/11	<b>410 to 920</b>	20	<b>80 to 480</b>	100	<b>10 to 0.4</b>		↓	↑	n	↓	[14]
PML B92/11	<b>370 to 960</b>	<b>16 to 20</b>	<b>60 to 240</b>	<b>24 to 8</b>	<b>1.5 to 0.5</b>		↓	↑	↑	n	[15]

1170

1171

1172

1173

1174

1175

1176

1177

1178

1179

1180

1181

1182

1183

1184

1185

1186

1187

1188

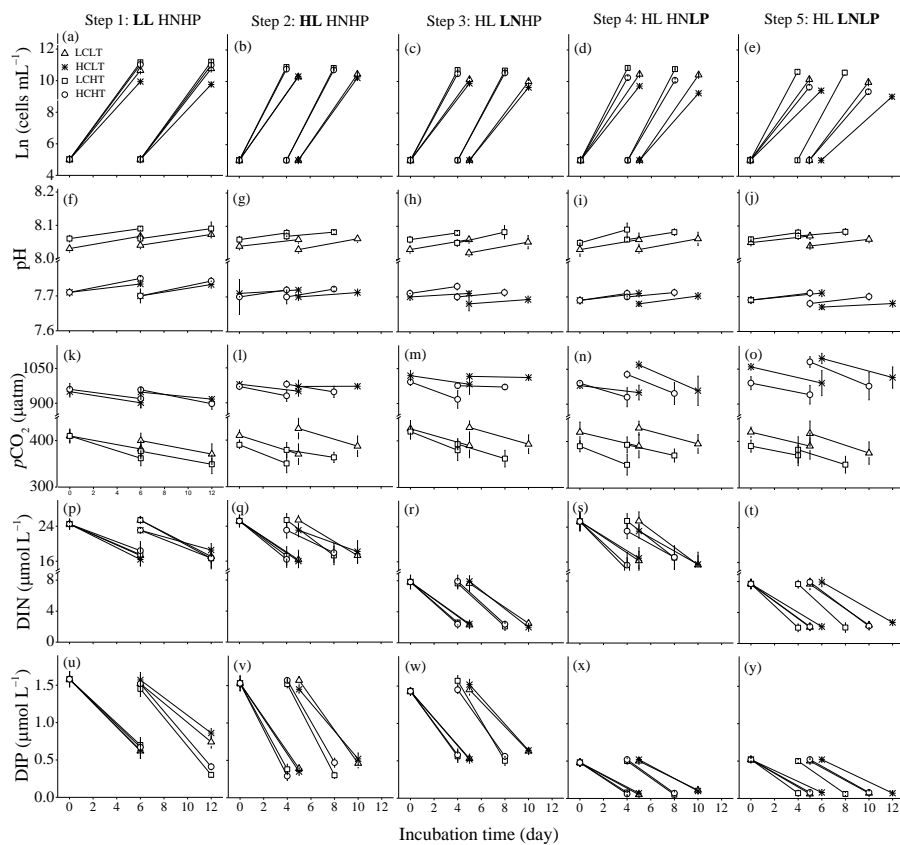
1189

1190



1191

1192



1193

1194

1195

1196

1197 Figure 1

1198

1199

1200

1201

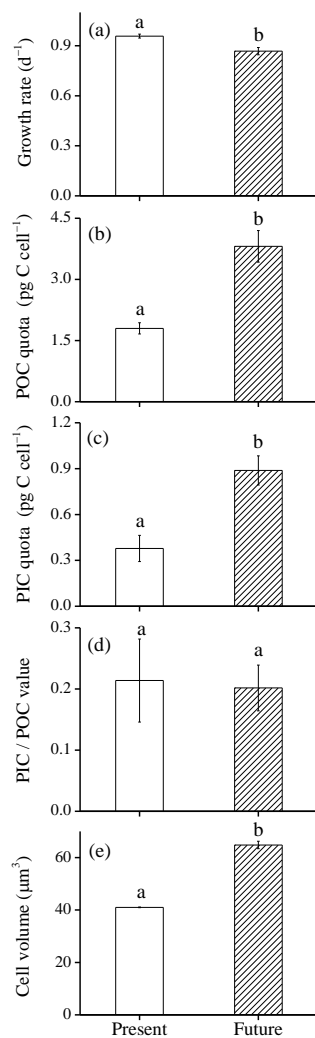
1202

1203



1204

1205



1206  
1207

1208

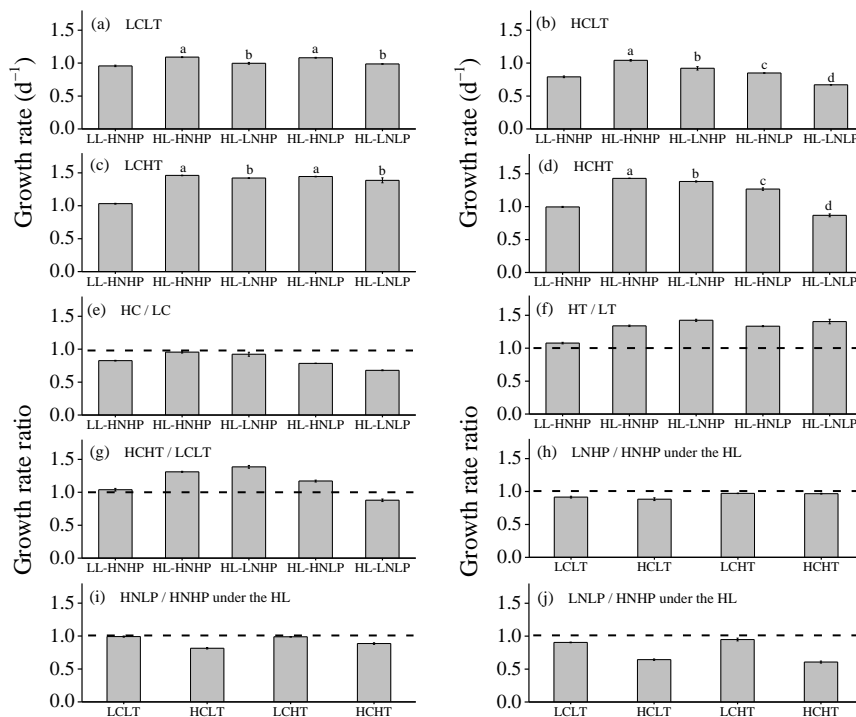
1209 Figure 2

1210



1211

1212



1213

1214

1215

1216

1217 Figure 3

1218

1219

1220

1221

1222

1223

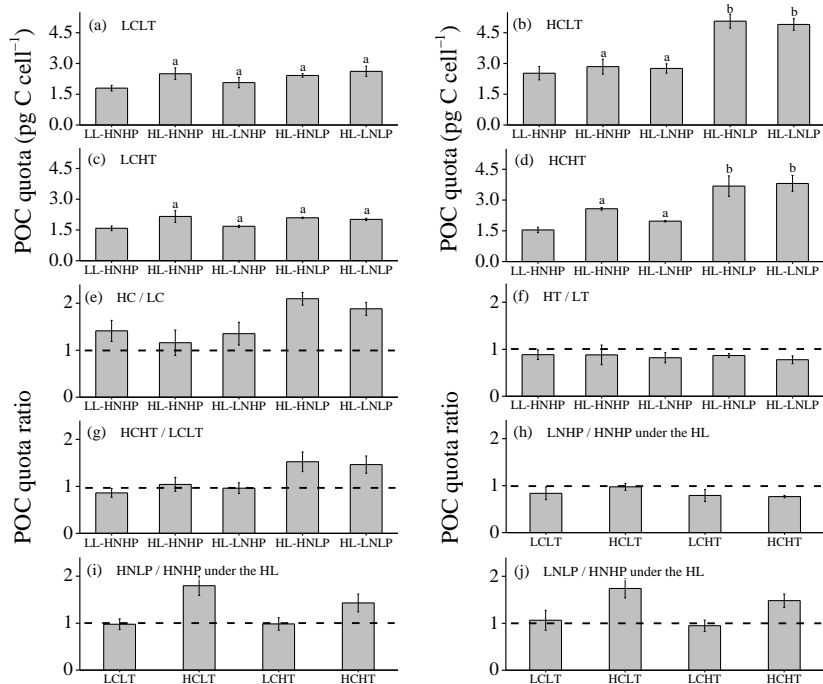
1224

1225



1226

1227



1228

1229

1230

1231

1232 Figure 4

1233

1234

1235

1236

1237

1238

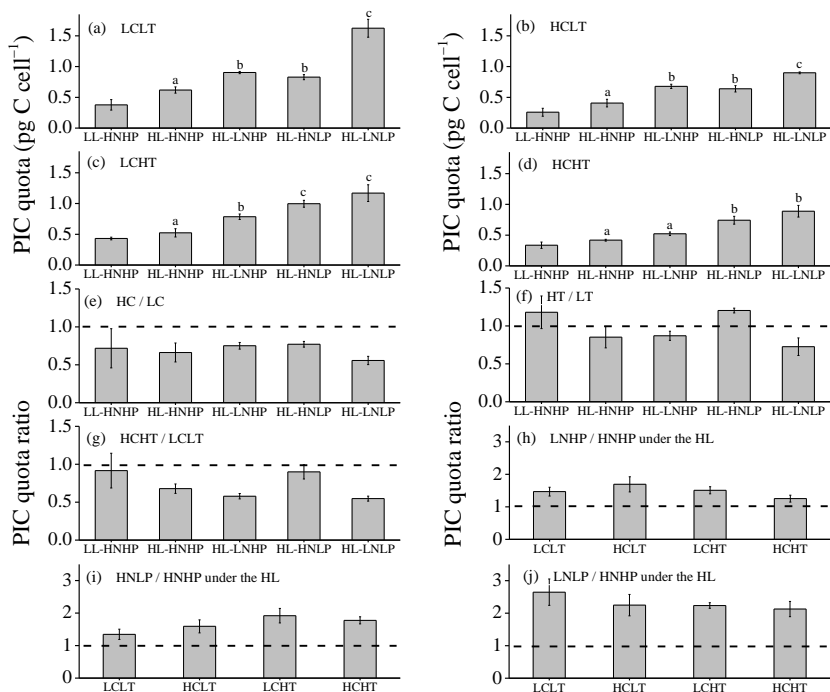
1239

1240



1241

1242



1243

1244

1245

1246

1247

1248 Figure 5

1249

1250

1251

1252

1253

1254

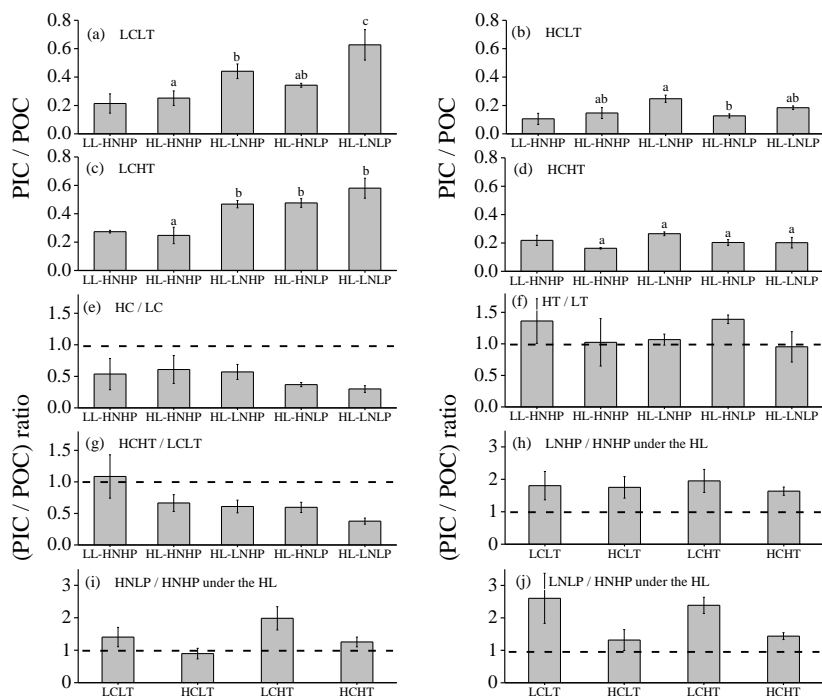
1255

1256



1257

1258



1259

1260

1261

1262

1263 Figure 6

1264

1265